

Semi-Autonomic AI LF-NMR Sensor for **Industrial** Profiling of Edible Oil Oxidation Status

Prof. Zeev Wiesman

Phyto-Lipid Biotech Lab (PLB)
Department of Biotech. Eng.
Ben Gurion University of the
Negev
Zeev.Wiesman@gmail.com



Semi-Autonomic AI LF-NMR Sensor for Industrial Prediction of Edible Oil Oxidation Status



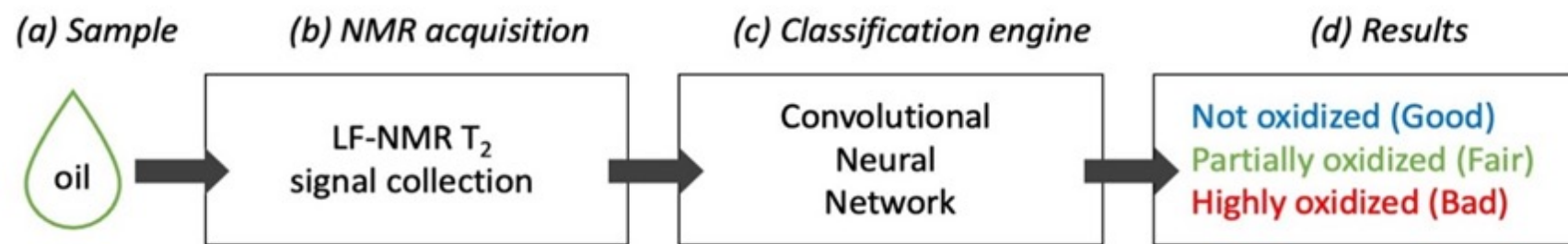
Abstract

Tatiana Osheter, Salvatore Campisi Pinto, Cristian Randieri, Andrea Perrotta, Charles Linder & Zeev Weisman*

The evaluation of an oil's oxidation status during industrial production is highly important with respect to monitoring the oil's purity and nutritional value, during production, transportation, storage, and cooking. The oil and food industry is seeking a real-time non-destructive, rapid, robust, and low-cost sensor for nutritional oil's material characterization.

Towards this goal, a ^1H LF-NMR relaxation sensor application based on chemical and structural profiling of non-oxidized and oxidized oils was developed and reported. This study deals with a relatively large-scale oil oxidation database which included crude data of a ^1H LF-NMR relaxation curve, and its reconstruction into T_1 and T_2 spectral fingerprints, self-diffusion coefficients D , and conventional standard chemical test results.

This study used a Convolutional Neural Network (CNN) that was trained to classify T_2 relaxation curves into three ordinal classes representing three different oil oxidation levels (non-oxidized, partial oxidation and high level of oxidation). Supervised learning was used on the T_2 signals paired with the ground-truth labels of oxidation values as per conventional chemical lab oxidation tests. The test data results (not used for training) show a high classification accuracy (95%). The proposed AI-based method is suitable for large training sets and food industry applications.





Aim:

To Develop a Facile Industrial AI-based Semi-Autonomic NMR Sensor Application to Rapidly Predict Oil-rich Food Products Safety and Quality.

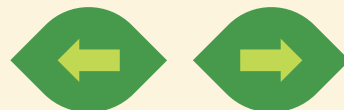
An Efficient Diagnostic Tool to Support Decision Makers in Food Industry

R&D:

Phase I – TD NMR sensorial 2D T1-T2 & D Chemical and Morphological Fingerprinting Pattern

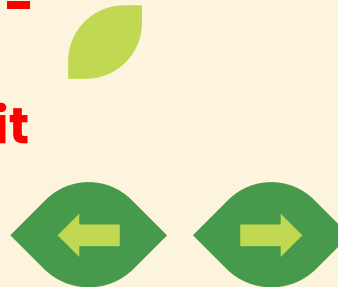
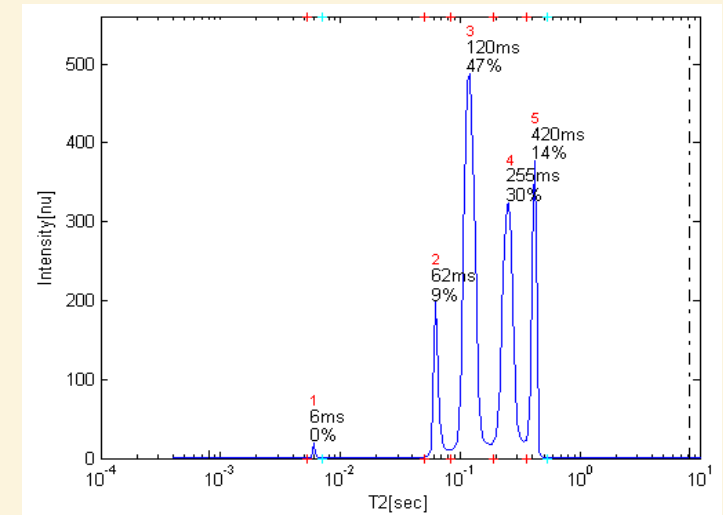
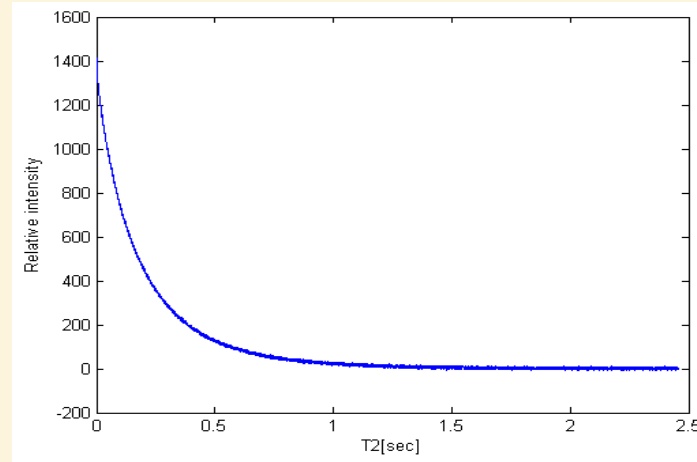
Phase II – TD NMR sensor Application for Determination of Oxidation Composition and Structural Fingerprints Changes

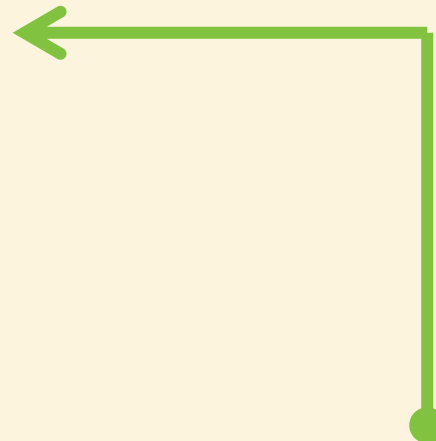
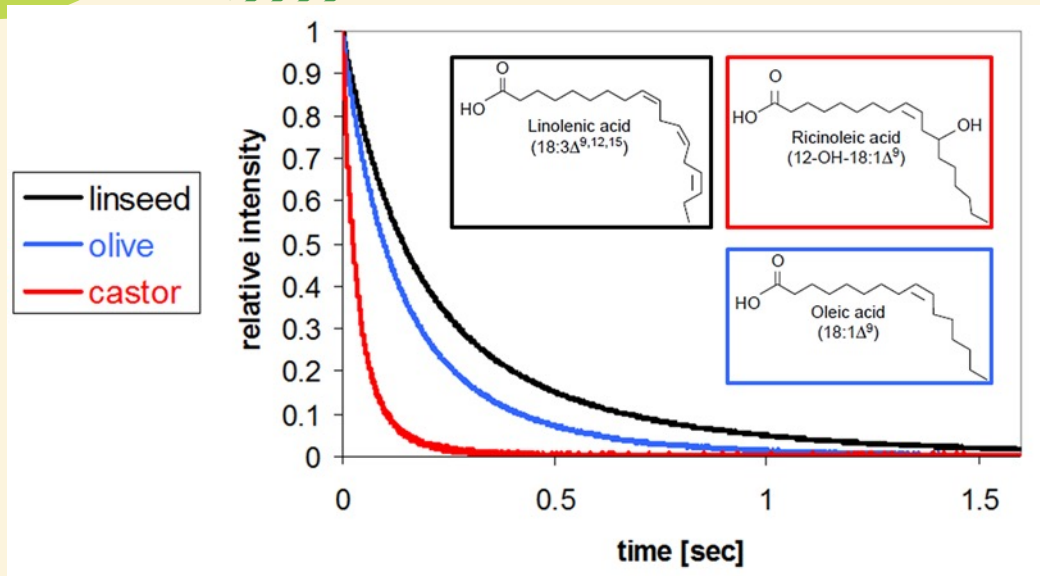
Phase III – AI-based Semi-Autonomic NMR Sensor Application for Profiling of Oil Oxidation Status



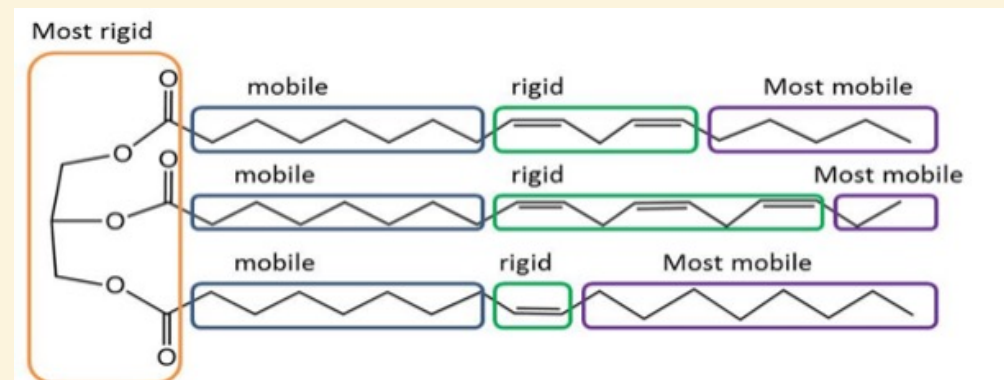
INTRODUCTION

- Low field ^1H NMR can generate relaxation times in less than 1 minute, by monitoring relaxation of ^1H magnetic spin after excitation
- With Inverse Laplace Transformation processing, relaxation curves can be transformed into T2 spectra
- T2 in previous studies – shows chemical and structural changes during oil oxidation
- Prior knowledge is needed to read these spectra, and processing takes time.
- **Goal of our study – to develop AI ^1H LF-NMR relaxation sensor for real-time evaluation of edible oil oxidation to fit the requirements of food industry to produce optimal food products without oil oxidation.**

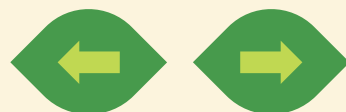


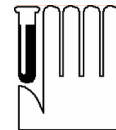


Effect of oils chemical composition and structure on LF-NMR T_2 relaxation curves. Linseed oil, olive oil and castor oil having different profile of unsaturated fatty acid and therefore different of structural organization, show different rate of proton relaxation curve.



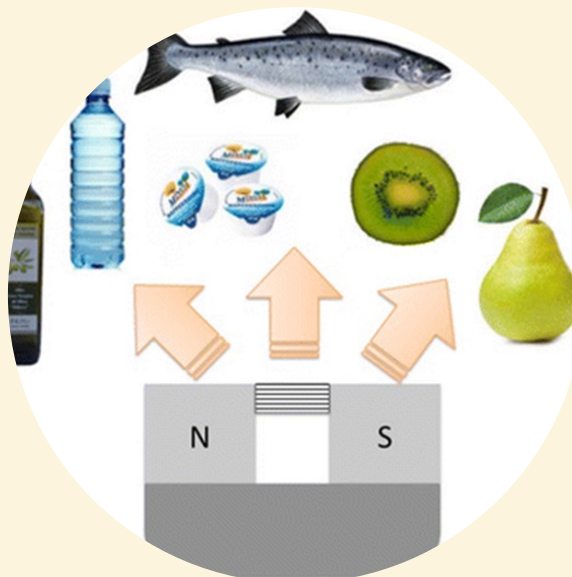
Scheme of triacylglycerol oil structure and segmental motion assigned by segmental rigidity mobility tests





***Intelligent TD NMR sensor** (principles and practice)

- Chemical and structural signature determination
- TD NMR guide for improved structure and texture
- Generation of big structure and texture signature **Pattern Recognition (PR) database**
- Machine Learning (ML) - **PR Modeling** of plant-based Milk & Meat signature recognition
- **Semi-Autonomic TD NMR sensor Decision Support System (DSS) for Safety & Health Value**



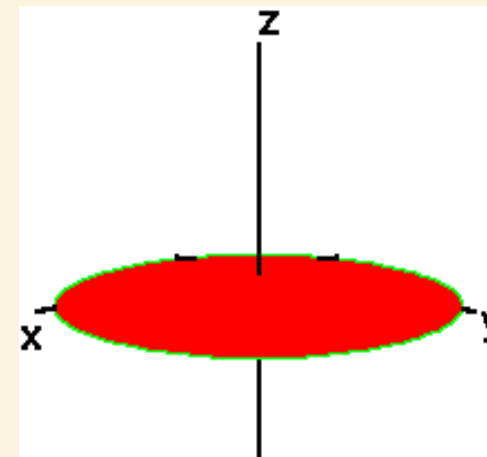
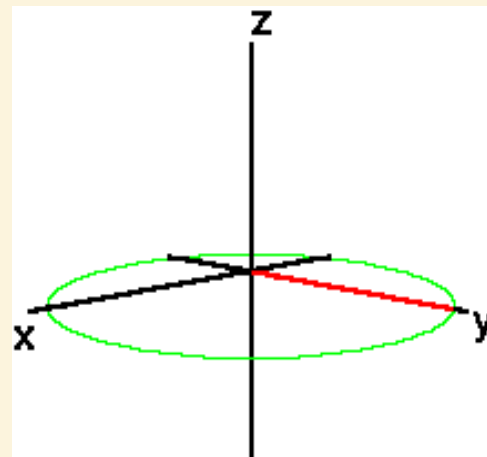
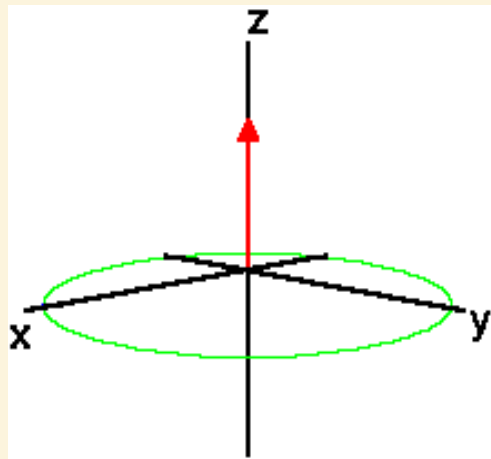
Relaxation Mechanisms



- After irradiation ceases, not only do the population of the states revert to a **Boltzmann distribution**, but also the individual nuclear magnetic moments begin to lose their phase coherence and return to a **random** arrangement around the z axis.
- The return of the equilibrium of the net magnetization is called “relaxation process”
- During relaxation, electromagnetic energy is retransmitted: this RF emission is called the NMR signal.

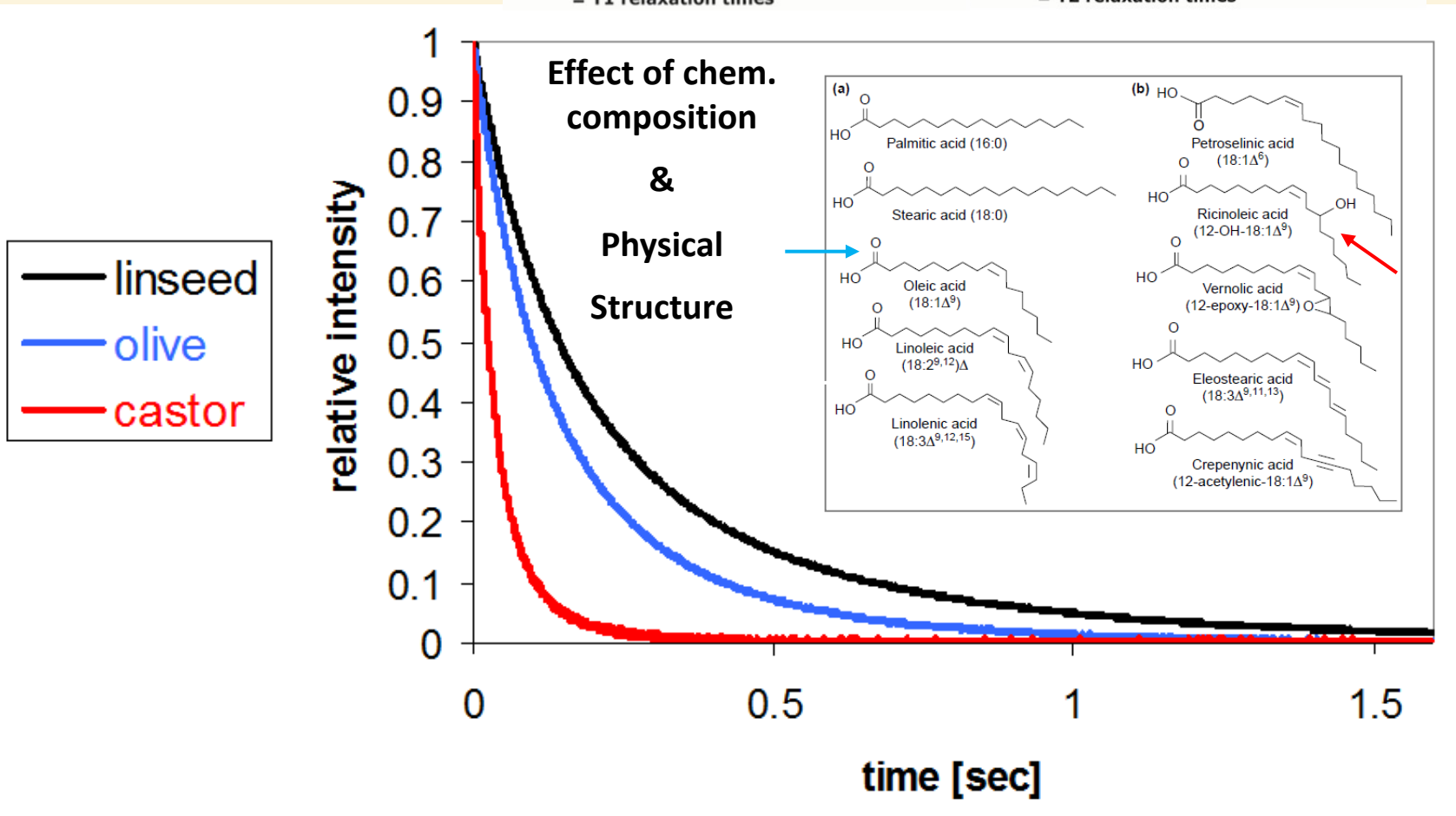
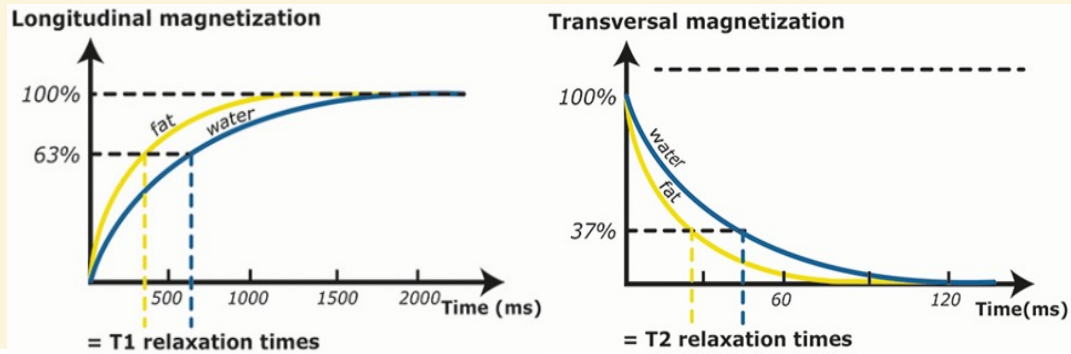
NMR spectroscopy record this process!!!

- There are two types of relaxation process : T1 (spin-lattice relaxation) & T2 (spin-spin relaxation)



^1H LF-NMR Relaxation Signals Collections & Chem. Composition & Physical Structure

Phase I - TD NMR Sensor

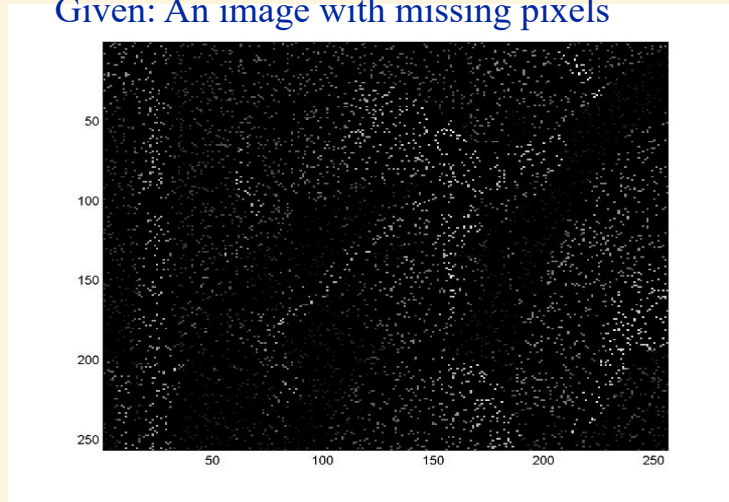


Inverse Laplace Transformation Solution for NMR SPARS Data based on PDCO



The 1D and 2D of T1 and T2 relaxation graphics required novel signal data analysis & intelligent computing approach for solving challenging **inverse problems in NMR Data processing**

Given: An image with missing pixels



The goal: Estimate the values of the missing pixels by 2D interpolation

The Challenge: Very high ratio of missing pixels, **standard near-neighbor interpolation scheme will fail**

PDCO - Primal Dual Interior method for Convex Objectives (Saunders, 2001; Berman et al 2013)

$$\begin{aligned} \min & \|Dw\|_2 \\ \text{s.t.} & Aw - x = 0 \\ & Jx = b \end{aligned}$$

PDCO based Solution

Where **A** is wavelets Dictionary
w is the 2D wavelets coeff.

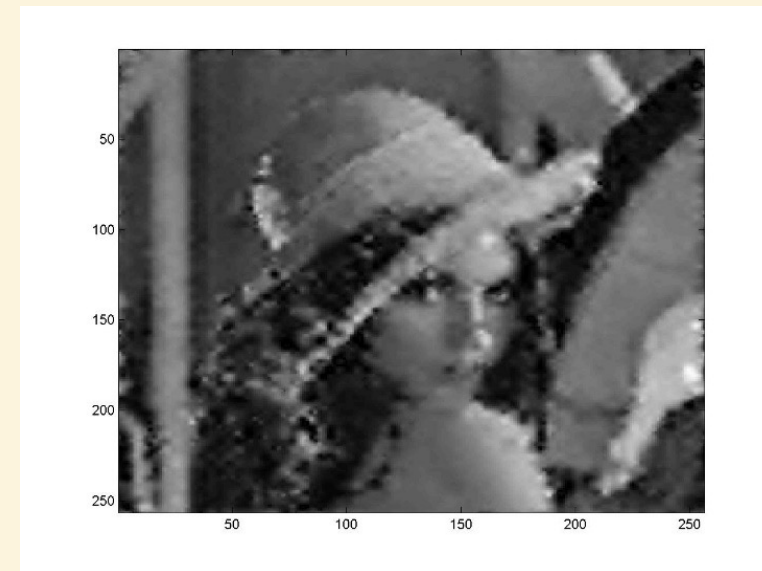
Vector **x** is the image pixels

Vector **J** is a row reduced identity matrix

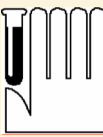
b is the vector of known pixels value

D is a diagonal positive matrix

Reconstruction result



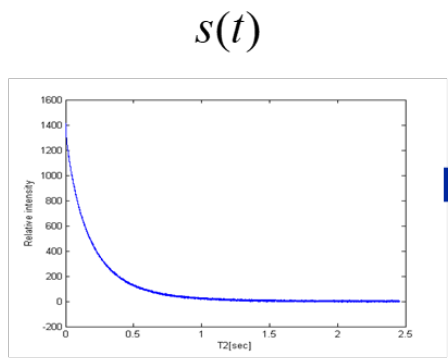
* Consideration of SNR – Signal to Noise Ratio
** Optimization of L1/L2 regularization parameters



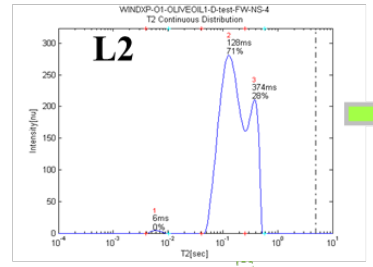
Phase I - PLBL Contribution for Optimization of ILT data processing

Using **optimal regularization parameters**, **PDCO solver** produce more detailed and accurate 1D T1 / T2 & 2D T1-T2 Structural **Fingerprints/Signature** in comparison to other available spectral solution (WinDXP & CONTIN) (confirmed by **simulation of results of real data**)

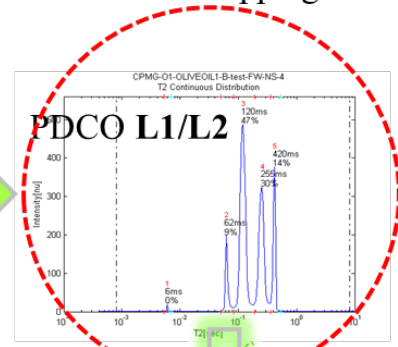
(1) MR Signal collection –
T2 Relaxation Curve S



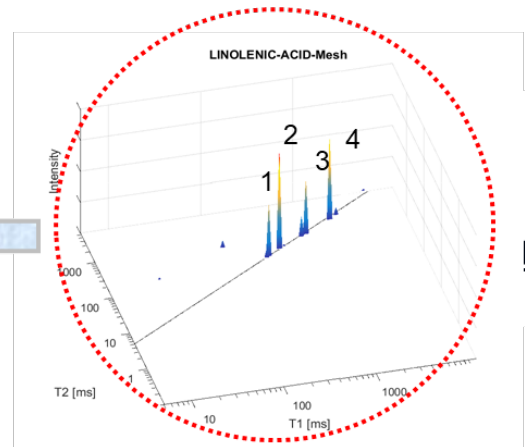
(2a) Data Processing –
ILT – **WinDXP** 1D
T2 Mapping



(2a'') **Improved ILT**
PDCO L1/L2 – 1D
T2 Mapping

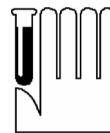


(3) **Lipid Products Dictionary** -
Time domain (TD) Peak Assignment
based on
Lipid Segmental Motion

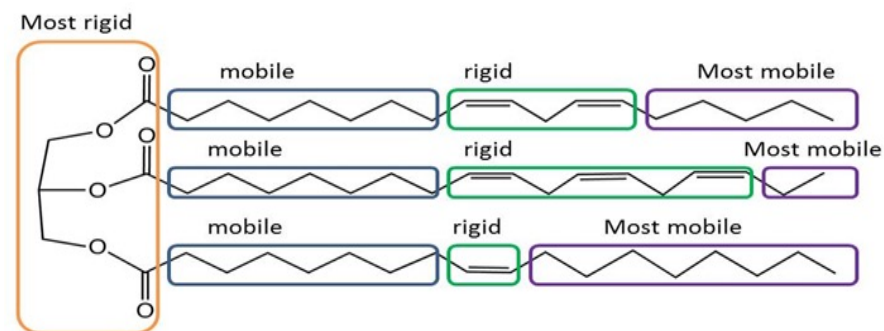
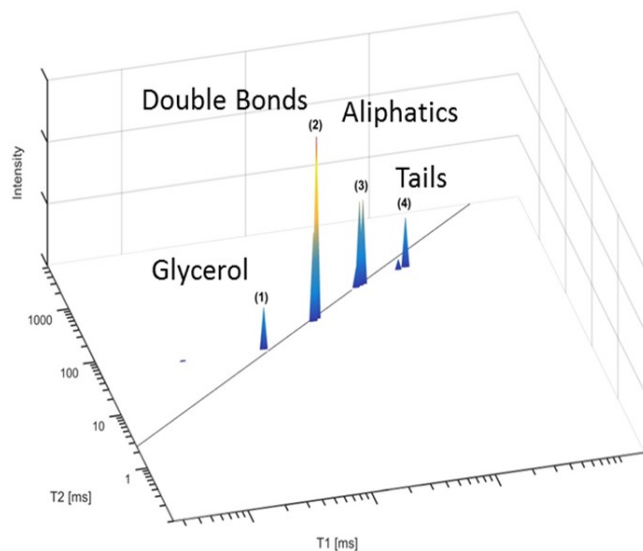


(2b) Data Processing –
PDCO L1/L2 ITL –
2D T1-T2 Mapping
Increased peak generation
and resolution

* Based on Resende et al 2018,2020; JAOCS



Demonstration of Segmental Motion TD NMR Sensor Fingerprint/Signature of Linseed Oil using PDCO Solver



Linseed oil chemical composition

FAs	%
16:0	5
16:1	1
18:0	4
18:1	20
18:2	15
18:3	55

Peak	T ₁ [ms]	T ₂ [ms]	Dictionary
1	94	53	Glycerol
2	191	135	Double bands
3	437	344	Aliphatic Chain
4	1003	766	Tail

* Based on Resende et al 2019; JLST

OIL OXIDATION

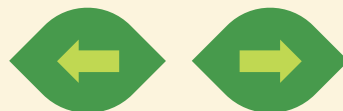


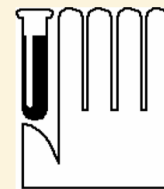
PUFA PARADOX

- Poly-unsaturated fatty acids (PUFA, includes $\Omega 3$), while considered beneficial to cardiovascular and neurological health, is sensitive to oxidation and creates carcinogenic by-products
- For this reason, PUFA-rich linseed oil is used in our study of monitoring oxidation

TESTING

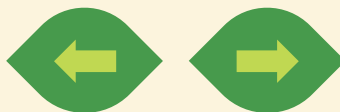
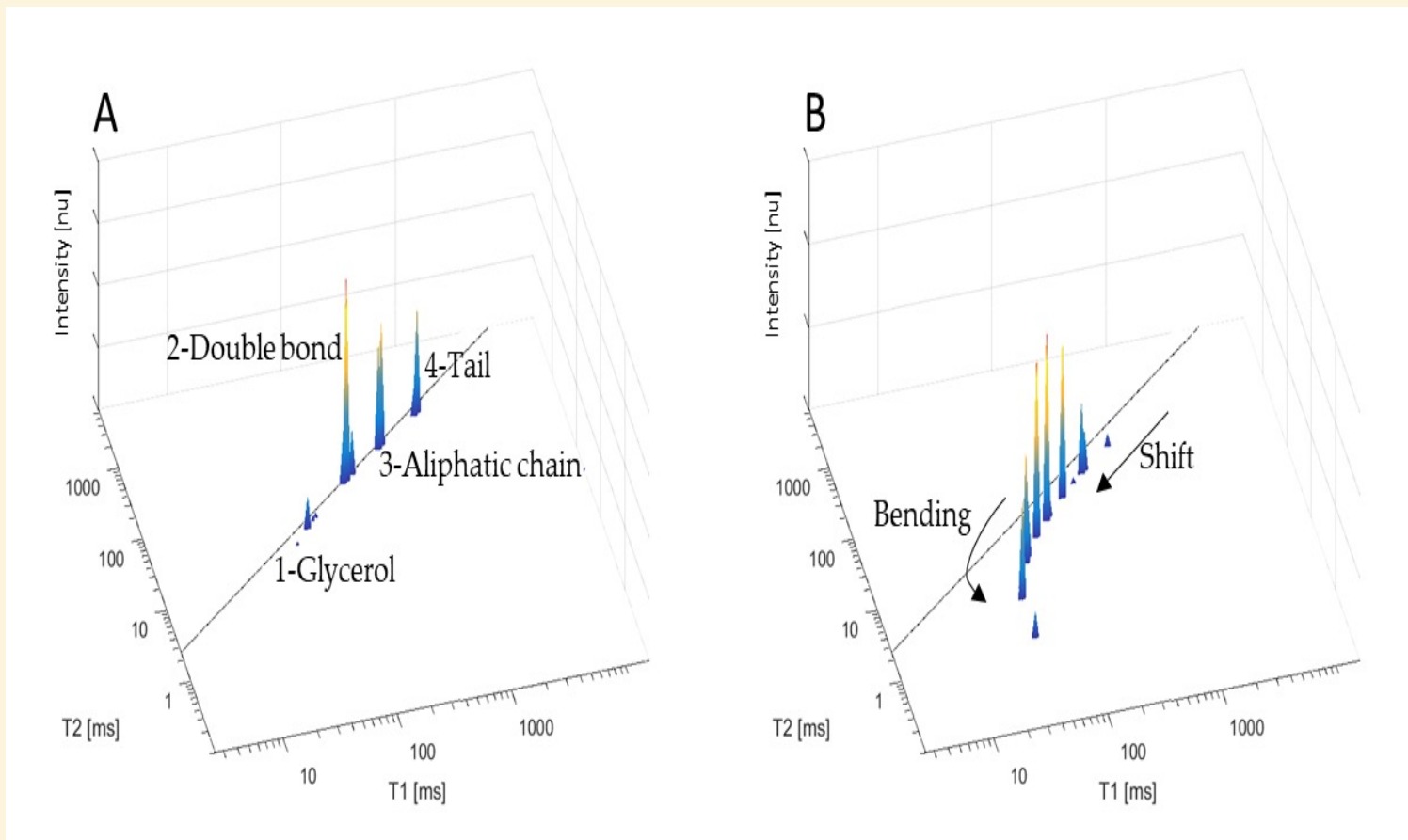
- 120 hours thermal oxidation induced by heating and air
 - Proton T2 relaxation analysis of oil samples in LF-NMR
 - Industry standard methods: peroxide value, *para*-anisidine value, TOTOX and self-diffusion coefficient D
- 285 Unique samples tested
- 3400 Data files

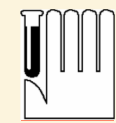




2D T_1 - T_2 chemical and morphological **TD NMR sensor** relaxation **FINGERPRINTS/SIGNATURE** of linseed oil before (A) and after 120 hours of thermal oxidation at 80°C plus air pumping (B).

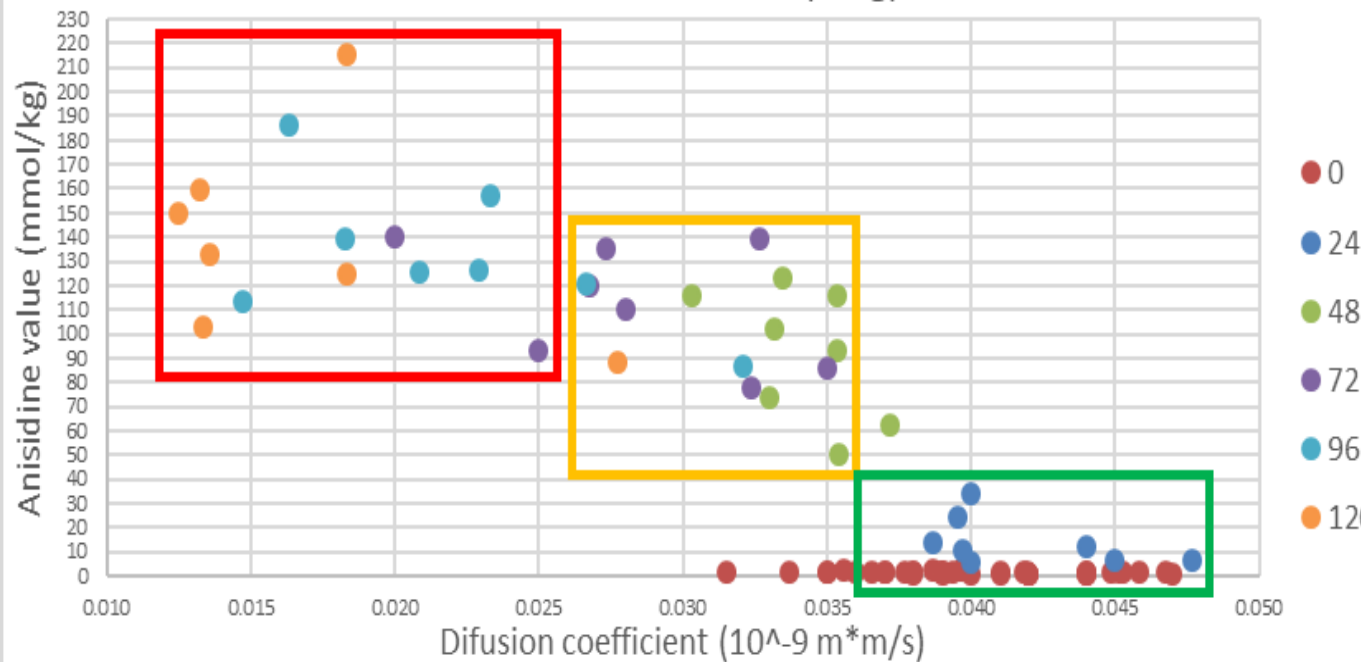
Each peak corresponds to a proton population motion in different segment of the linseed oil.





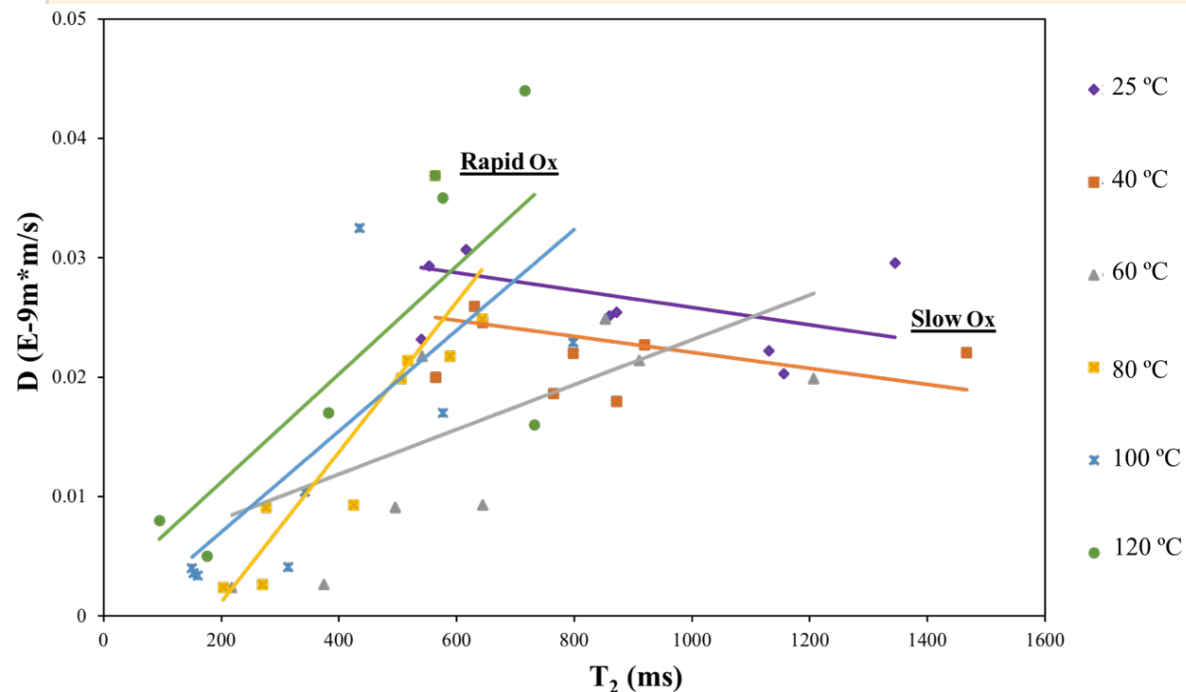
Correlations of parameters corresponding with oxidation

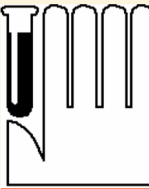
Anisidine value vs diffusion coefficient (avrg) on different ox times



Correlation between LSO self-diffusion coefficient (proton mobility in LF-NMR sensor) and conventional standard chemical tests (p-anisidine test) induced by thermal oxidation for different time (0, 25, 40, 60, 80, 100, 120 hrs). Using these tests, three levels of oxidation were classified: **GREEN – GOOD OIL**; **YELLOW – MEDIUM OIL**; **RED – VERY BAD OIL**

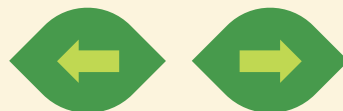
Correlation between LSO self-diffusion coefficient and T_2 at 25, 40, 60, 80, 100, 120 °C during 168 h. (25 and 40 °C designated as Slow Ox and 60, 80, 100, 120 °C designated as Rapid Ox)





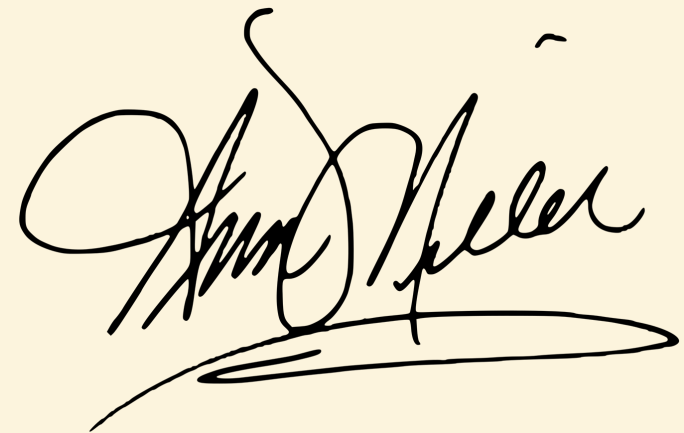
Criteria for dividing oil samples to the following three categories:
'Good', 'Fair' and 'Bad'.

Category	NMR coefficient D range (*10 ⁻⁹ m ² /s)	Chem. standard PV range (mmol/kg)	Total samples
'Good'	> 0.03	< 20	126
'Fair'	0.02 - 0.03	20 - 50	77
'Bad'	≤ 0.02	≥ 50	187

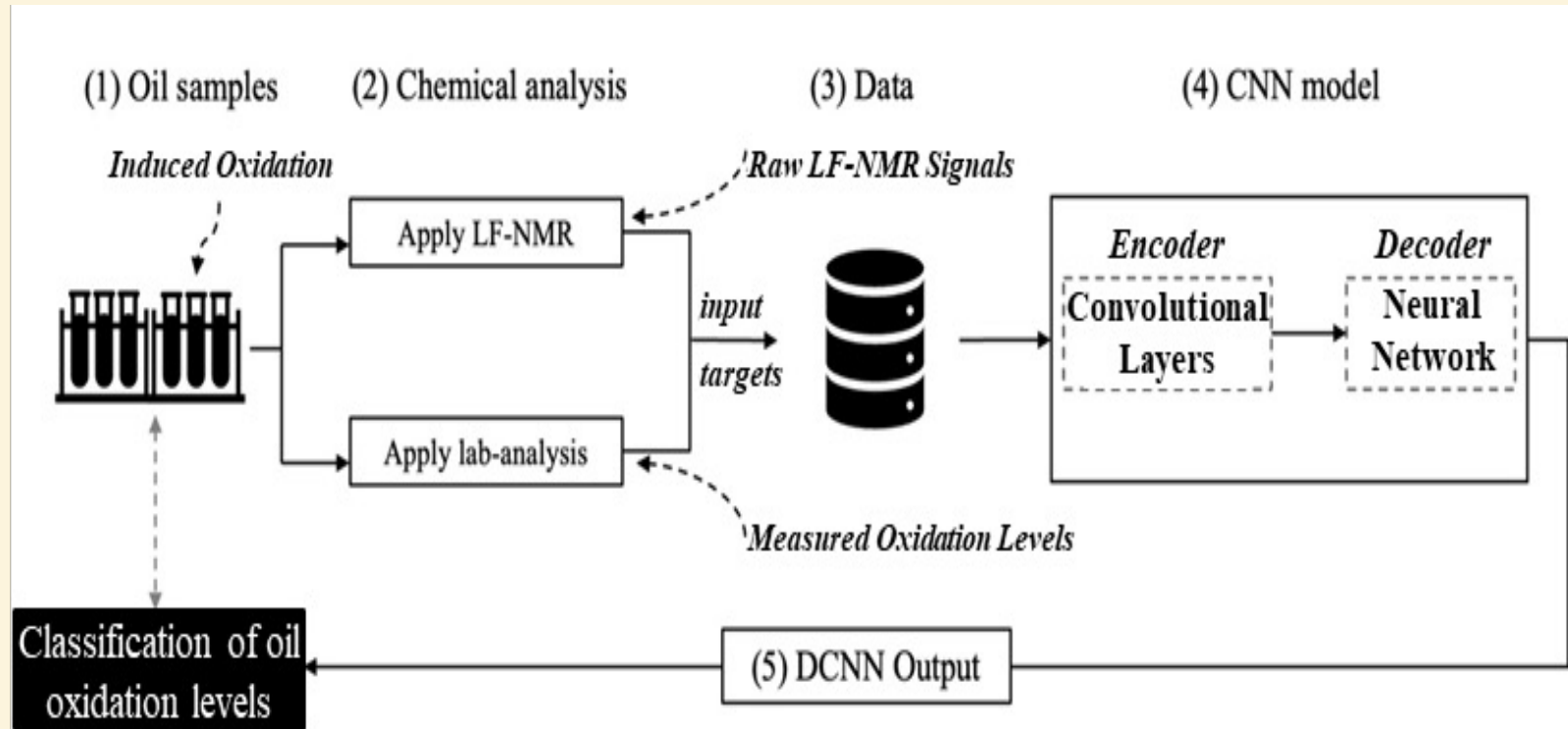




**Browser
Fingerprinting:
A Complete Guide**

A laptop displaying a fingerprint icon on its screen.

Machine Learning Model Concept



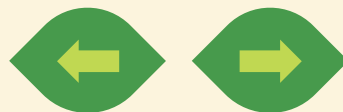
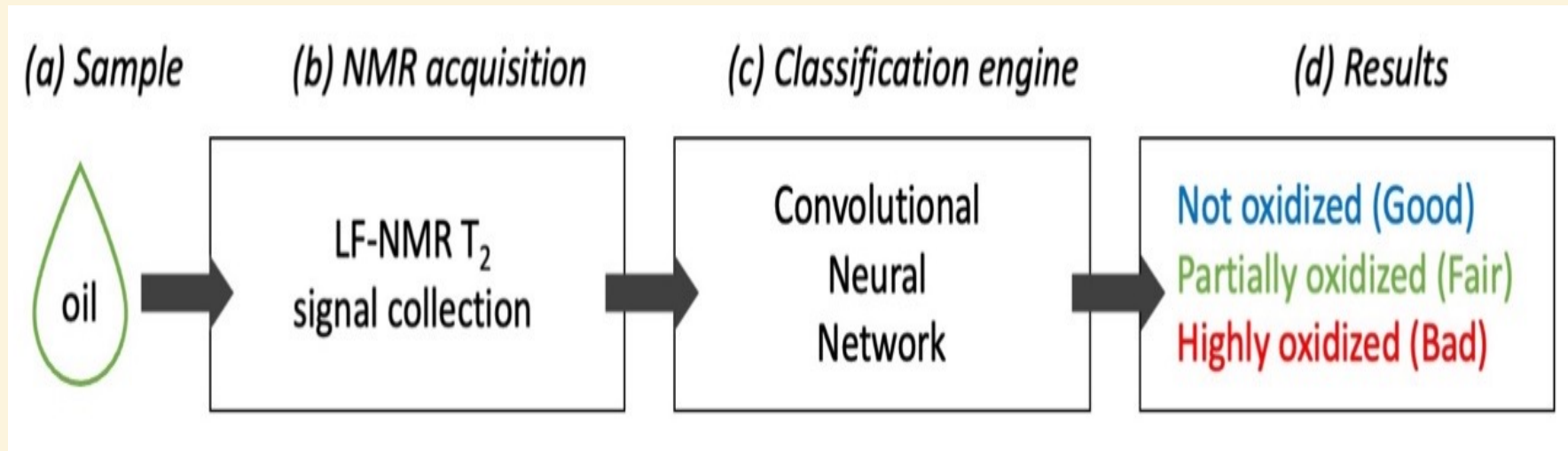
Training and testing system for machine learning: oil samples (1) are analyzed via LF-NMR and conventional lab methods (2) these are combined into a data-frame of inputs and targets (3) for supervised learning via CNN (4); deep convolution neural network (DCNN) output i.e. classification of T_2 signals into oxidation classes (5) are benchmarked against ground truth measurements in order to assess prediction accuracy and to fine-tune the system in a series of recursive cycles until satisfactory accuracy is achieved. Having concluded system fine-tuning and training, the trained CNN is ready for deployment.





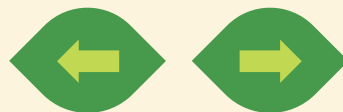
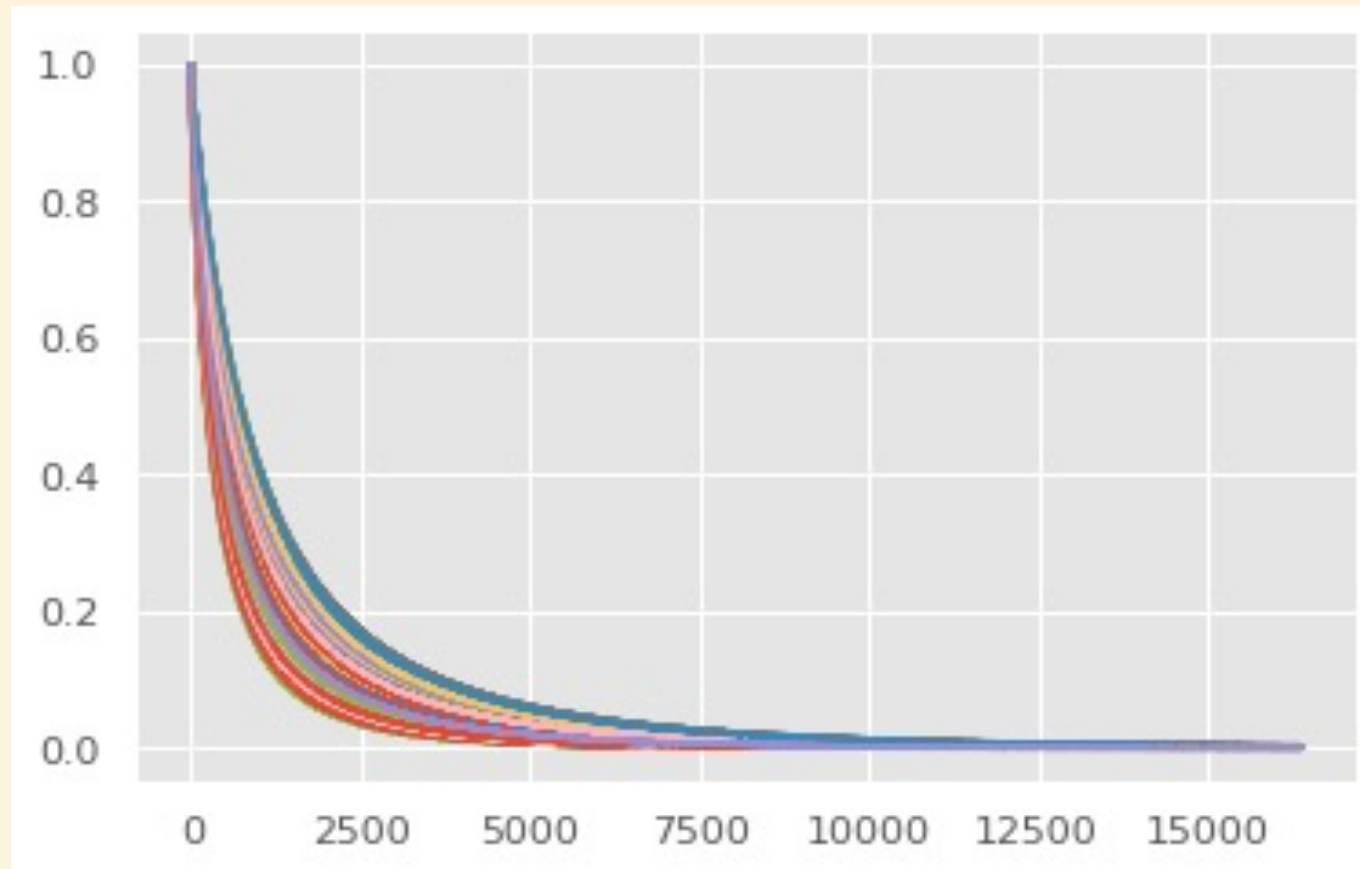
Convolution Neural Network (CNN)

System set up, a typical workflow where a drop of oil is scanned with a LF-NMR magnetometer; in the next step the CNN uses the **T₂ signals as an input** and return the **oil oxidation class as output**.

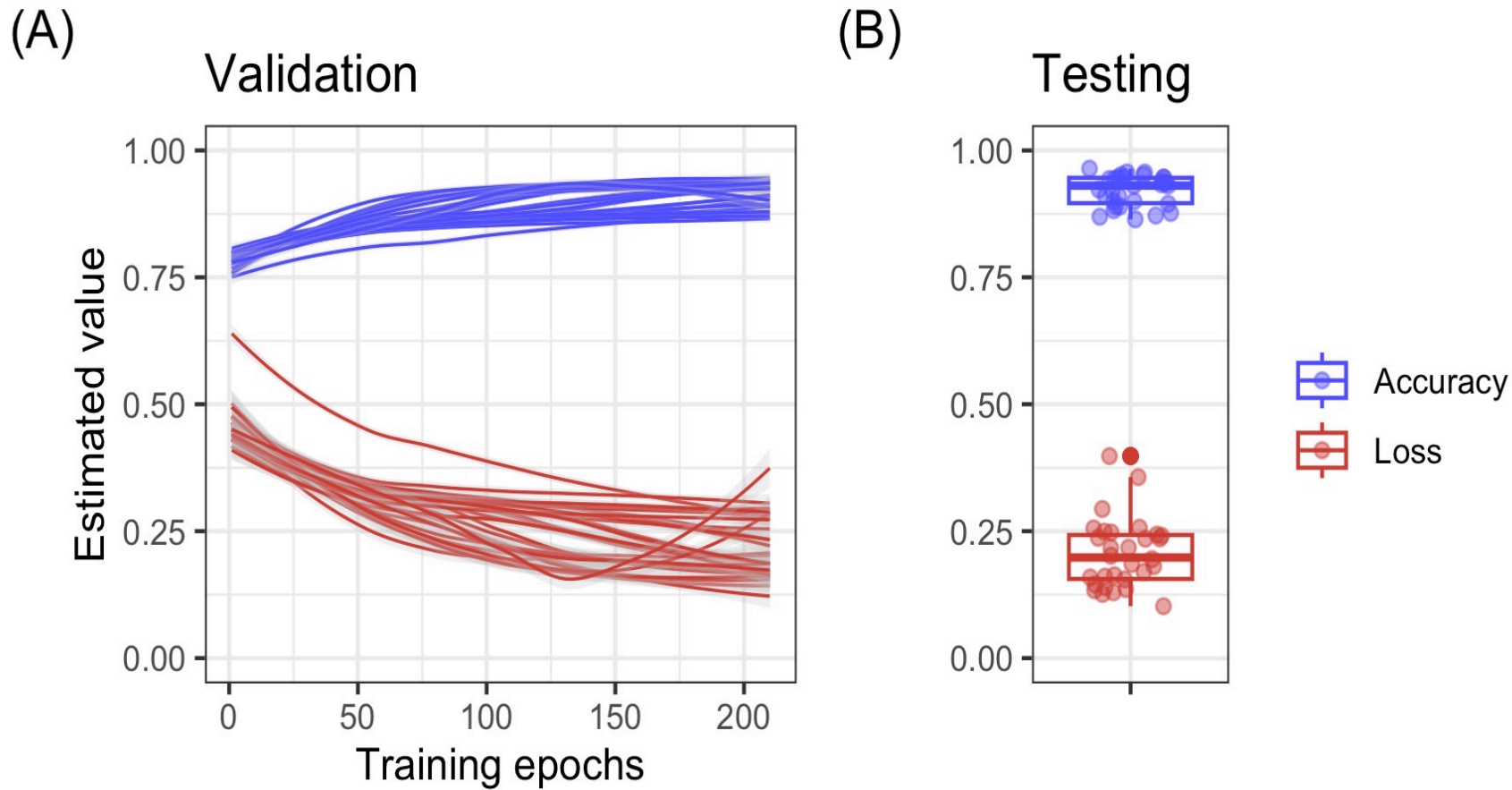




LF NMR T_2 relaxation time of thermal induced linseed oil samples oxidation. Each line color represents from top to bottom T_2 relaxation time (0hr, 12hr, 24hr, 48hr, 96hr, 120hr).
(AI machine differentiates between lines much better than human eyes/brain)



Accuracy and Loss function over a typical training session, values are estimated over both training and validation data.



Accuracy and loss functions for 30 different convolutional neural network (CNN) training sessions. (A) refers to the validation set; it shows how accuracy and loss evolve over time; typically accuracy increases and loss decreases over epochs. (B) shows the final performances on the testing set (a subset of data that was not used for training). Data indicate that both validation and testing performances remain homogeneous over multiple ($n = 30$) randomly initiated training sessions, indicating that the CNN is properly tuned, the architecture is appropriate for the data, and performances are replicable.



Convolutional neural network test performances by oxidation class.

	Oxidation class			
	Bad	Fair	Good	Overall
Number of repetitions (n)	30	30	30	30
Support (n of samples)	126	77	187	390
Total number of tests	3780	2310	5610	11,700
Precision (%) (median, [IQR ¹])	97% [87%, 0.98%]	88% [84%, 90%]	94% [93%, 96%]	93% [87%, 96%]
Recall (%) (median, [IQR ¹])	98% [96%, 100%]	77% [59%, 83%]	97% [96%, 98%]	96% [83%, 98%]
F1-score (median, [IQR ¹])	0.96 [0.91, 0.98]	0.81 [0.69, 0.86]	0.96 [0.95, 0.97]	0.95 [0.86, 0.96]

¹ IQR = Interquartile range.



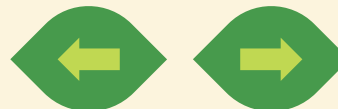
THE MODEL

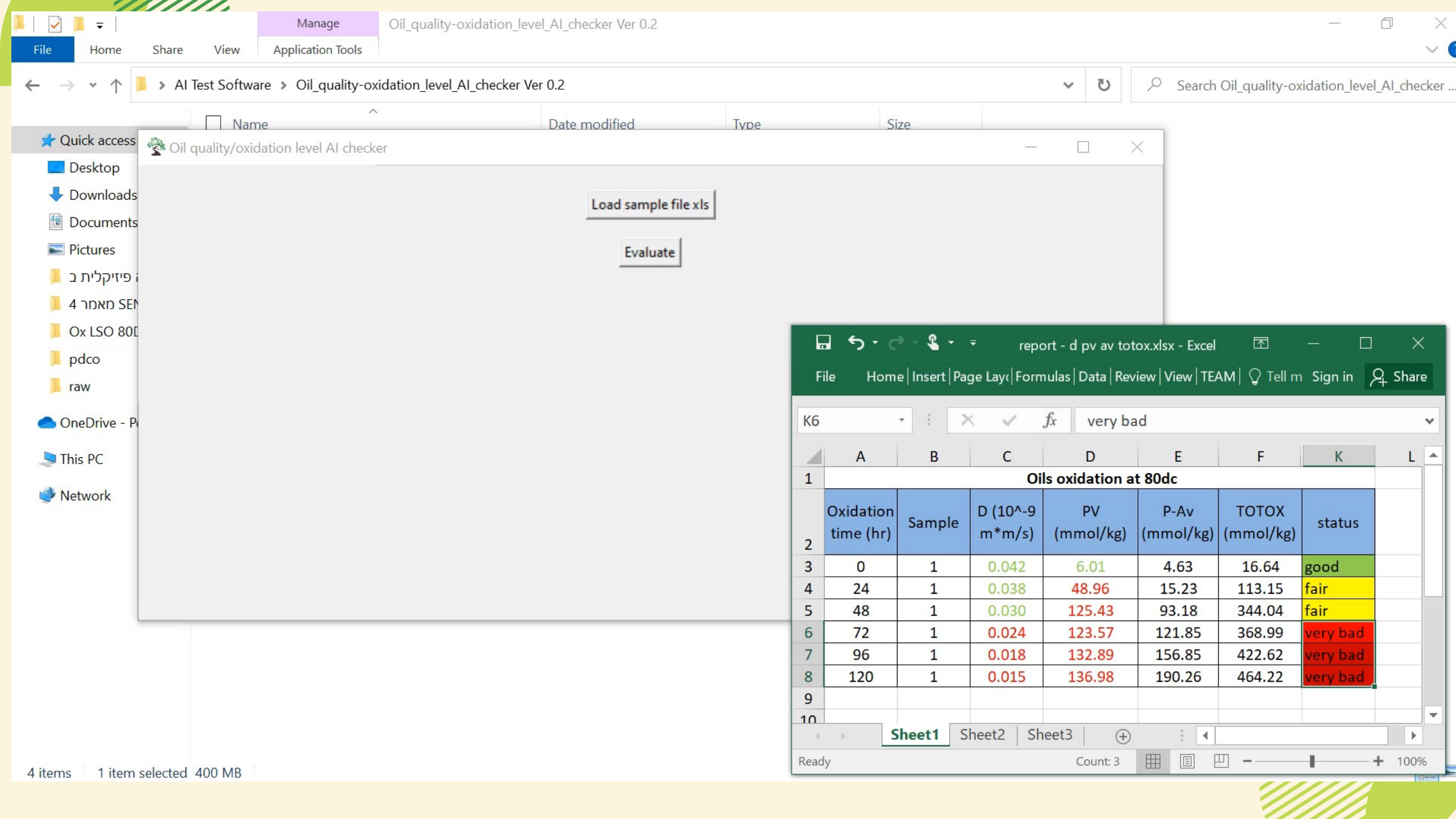
Supervised learning to train a CNN for classifying linseed oil T2 relaxation curves into three classes that reflect three oil oxidation levels (determined via standard methods) – **Good/Medium/Bad**



PERFORMANCES METRICS

The precision of identifying Good, Fair and Bad oil is 94%, 88% and 97%. In average, the classification accuracy of our model is **96%**





Oil quality/oxidation level AI checker

Load sample file xls

Evaluate

report - d pv av totox.xlsx - Excel

File Home Insert Page Layout Formulas Data Review View TEAM Tell me Sign in Share

K6 very bad

	A	B	C	D	E	F	K	L	
1	Oils oxidation at 80dc								
2	Oxidation time (hr)	Sample	D (10⁻⁹ m*m/s)	PV (mmol/kg)	P-Av (mmol/kg)	TOTOX (mmol/kg)	status		
3	0	1	0.042	6.01	4.63	16.64	good		
4	24	1	0.038	48.96	15.23	113.15	fair		
5	48	1	0.030	125.43	93.18	344.04	fair		
6	72	1	0.024	123.57	121.85	368.99	very bad		
7	96	1	0.018	132.89	156.85	422.62	very bad		
8	120	1	0.015	136.98	190.26	464.22	very bad		
9									
10									

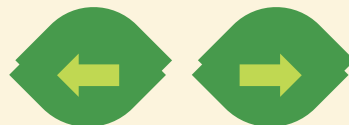
Sheet1 Sheet2 Sheet3

Ready Count: 3 100%



FUTURE PLANS

- Further improving accuracy (>96%) by further machine training.
- Applying specific modified AI CNN model to other industrial fields and processes (“Petroleum”).
- Industrial pilot demonstration.





Acknowledgements



PLBL members:


Prof. Zeev Wiesman
Dr. Janna
Abramovich
Dr. Maysa T Resende
Tatiana Osheter
Shoshana Kravchik
Alexey Osheter
Meir Cohen
Paula Berman
Nitzan Meiri
Natan Ayalon
Rotem Zamir
Eng. Project Students

Collaborators:

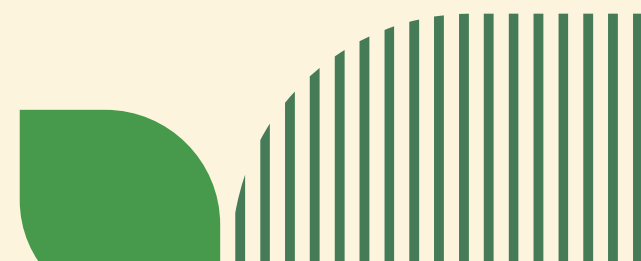
Prof. Cristian Randieri –
eCampus U
Prof. Charles Linder – BGU
Prof. Niva Shapira – AAC
Dr. Ofer Levi – OPU
Dr. Salvador Campisi-Pinto –
BGU
Dr. Yisrael Parmet –BGU
Prof. Michael Saunders –
Stanford U
Dr. Brian Hills – UK
Prof. Robert Glaser – BGU
Dr. Luiz Alberto Colnago – Brazil
Dr. Dimitri Mogliansk – BGU
Mrs. Sharon Hazan – BGU
Dr. Mark Karpasas – BGU

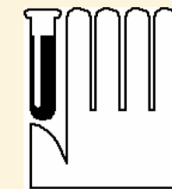
Sponsors:

Ormat Technologies
Israeli Ministry of
Science and
Technology & Space
Israeli Ministry of
Energy and Water
Israeli Ministry of
Environment
Protection
Israeli Authority of
Innovation
Good Food Institute
(GFI)

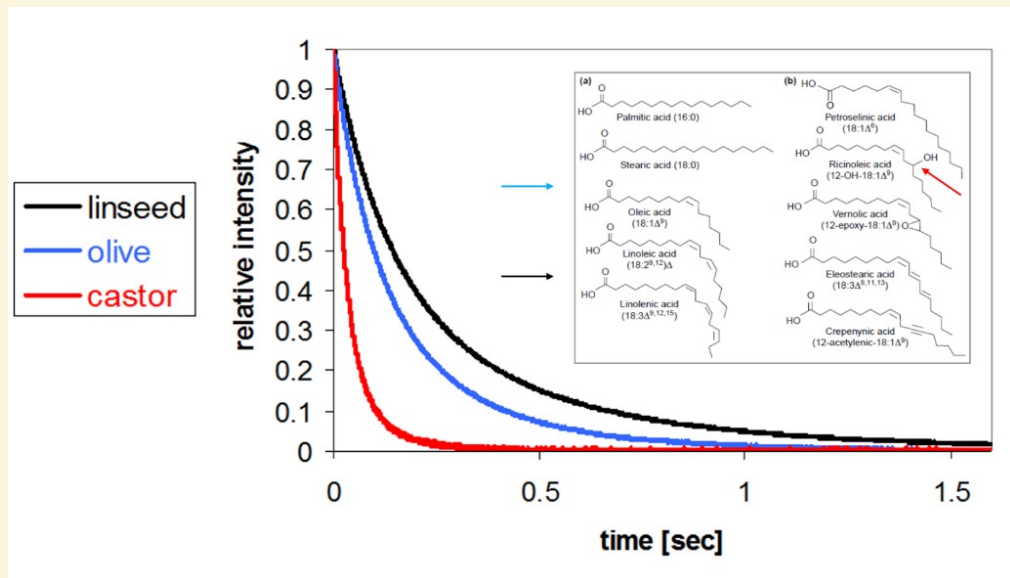
A collection of decorative green shapes in the top right corner, including a light green semi-circle, a dark green semi-circle, a pattern of horizontal lines, and a light green semi-circle.

Appendix

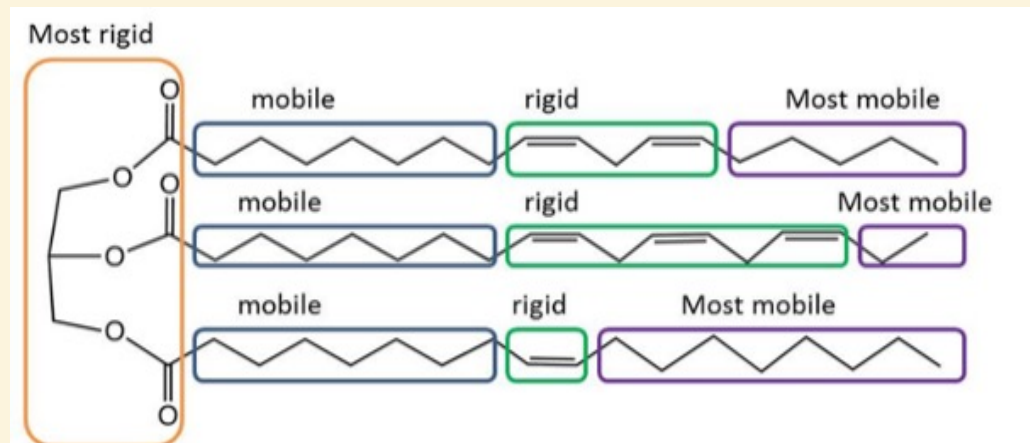
A collection of decorative green shapes in the bottom right corner, including a dark green semi-circle, a pattern of vertical lines, and a light green semi-circle.A large, solid green rounded rectangle occupies the left side of the page, with a small dark green leaf shape at its top left corner.A green shape with diagonal stripes is located at the bottom left, partially overlapping the large green rounded rectangle.



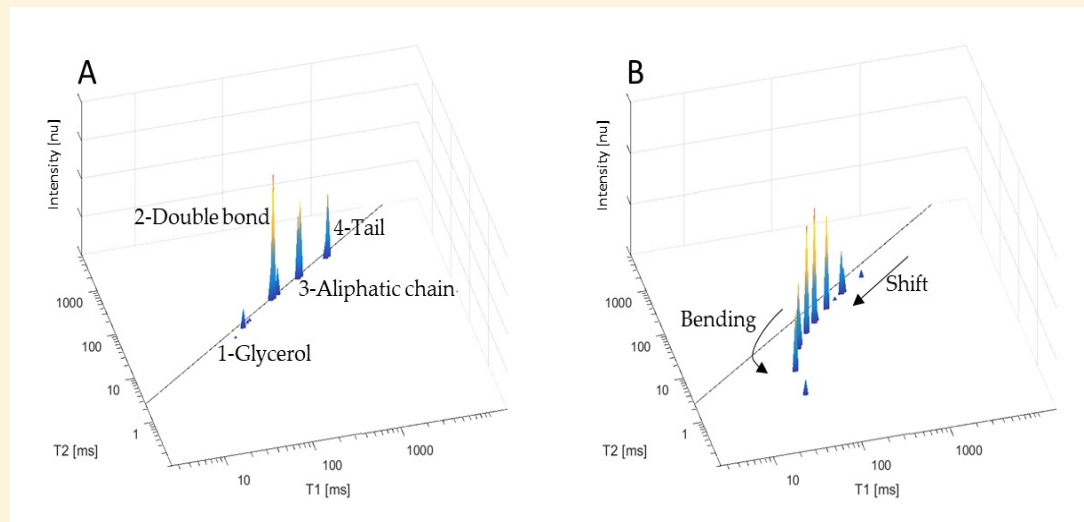
Effect of oils chemical composition and structure on LF-NMR T_2 relaxation curves. Linseed oil, olive oil and castor oil having different profile of unsaturated fatty acid and therefore different of structural organization, show different rate of proton relaxation curve.

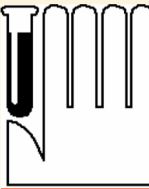


Scheme of triacylglycerol oil structure and segmental motion assigned by segmental rigidity mobility tests.

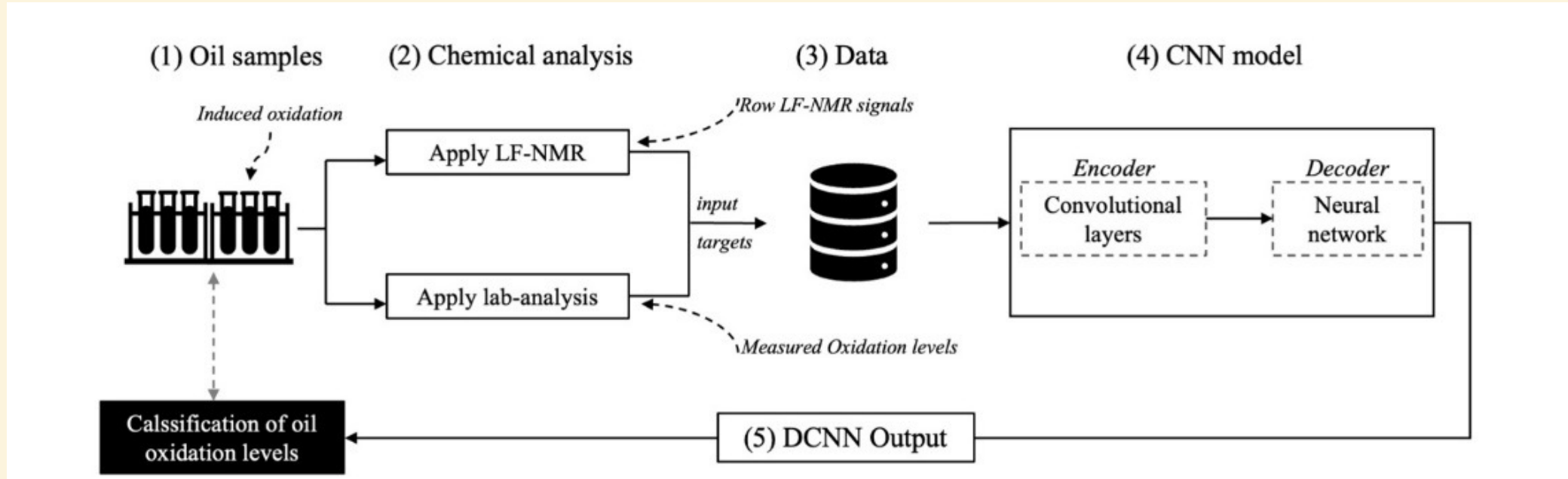


Chemical and morphological time domain NMR sensor 2D T_1 - T_2 relaxation times of linseed oil before (A) and after 120 hours of thermal oxidation at 80°C plus air pumping (B). Each peak corresponds to a proton population motion in different segment of the linseed oil.





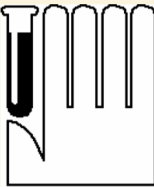
Training and testing system for machine learning: oil samples (1) are analyzed via LF-NMR and conventional lab methods (2) these are combined into a data-frame of inputs and targets (3) for supervised learning via CNN (4); deep convolution neural network (DCNN) output i.e. classification of T_2 signals into oxidation classes (5) are benchmarked against ground truth measurements in order to assess prediction accuracy and to fine-tune the system in a series of recursive cycles until satisfactory accuracy is achieved. Having concluded system fine-tuning and training, the trained CNN is ready for deployment.



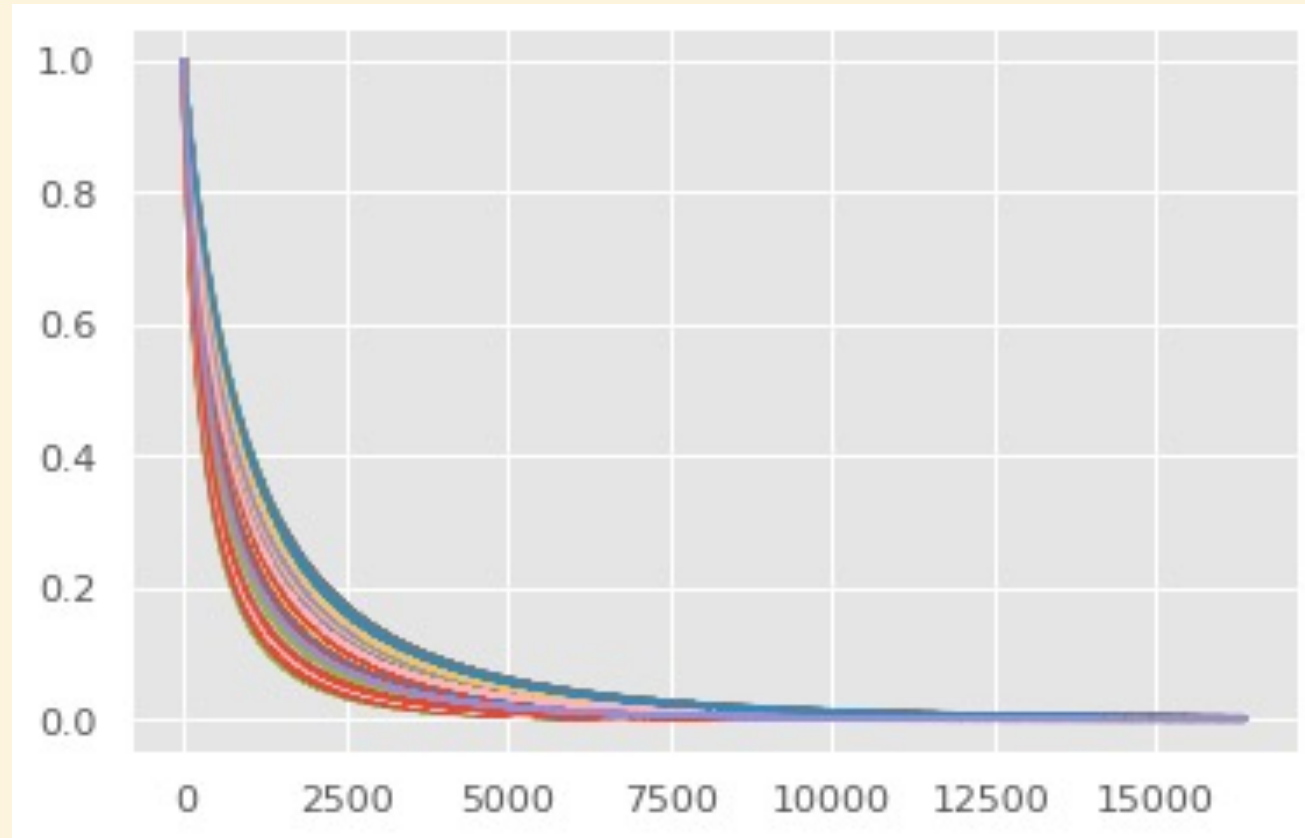


Criteria for dividing oil samples to the following three categories: 'Good', 'Fair' and 'Bad'.

Catergory	D range (*10⁻⁹ m²/s)	PV range (mmol/kg)	Total samples
'Good'	> 0.03	< 20	126
'Fair'	0.02 - 0.03	20 - 50	77
'Bad'	≤ 0.02	≥ 50	187

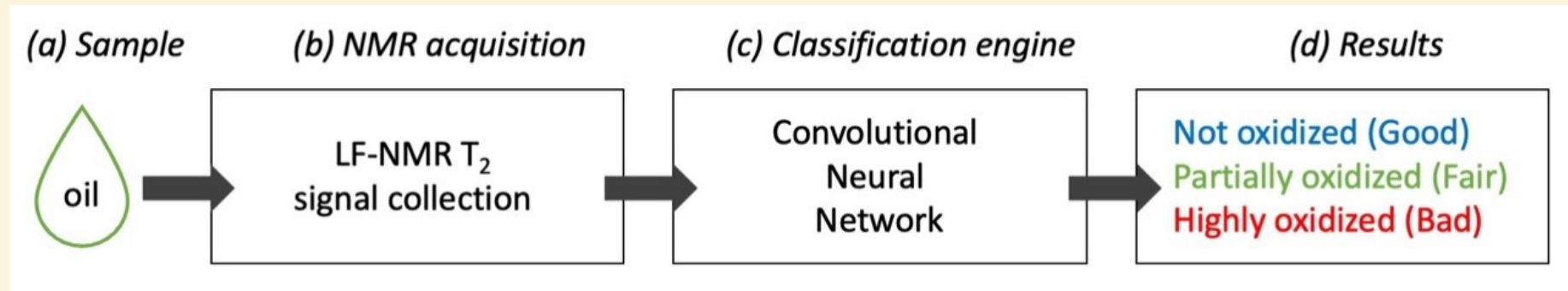


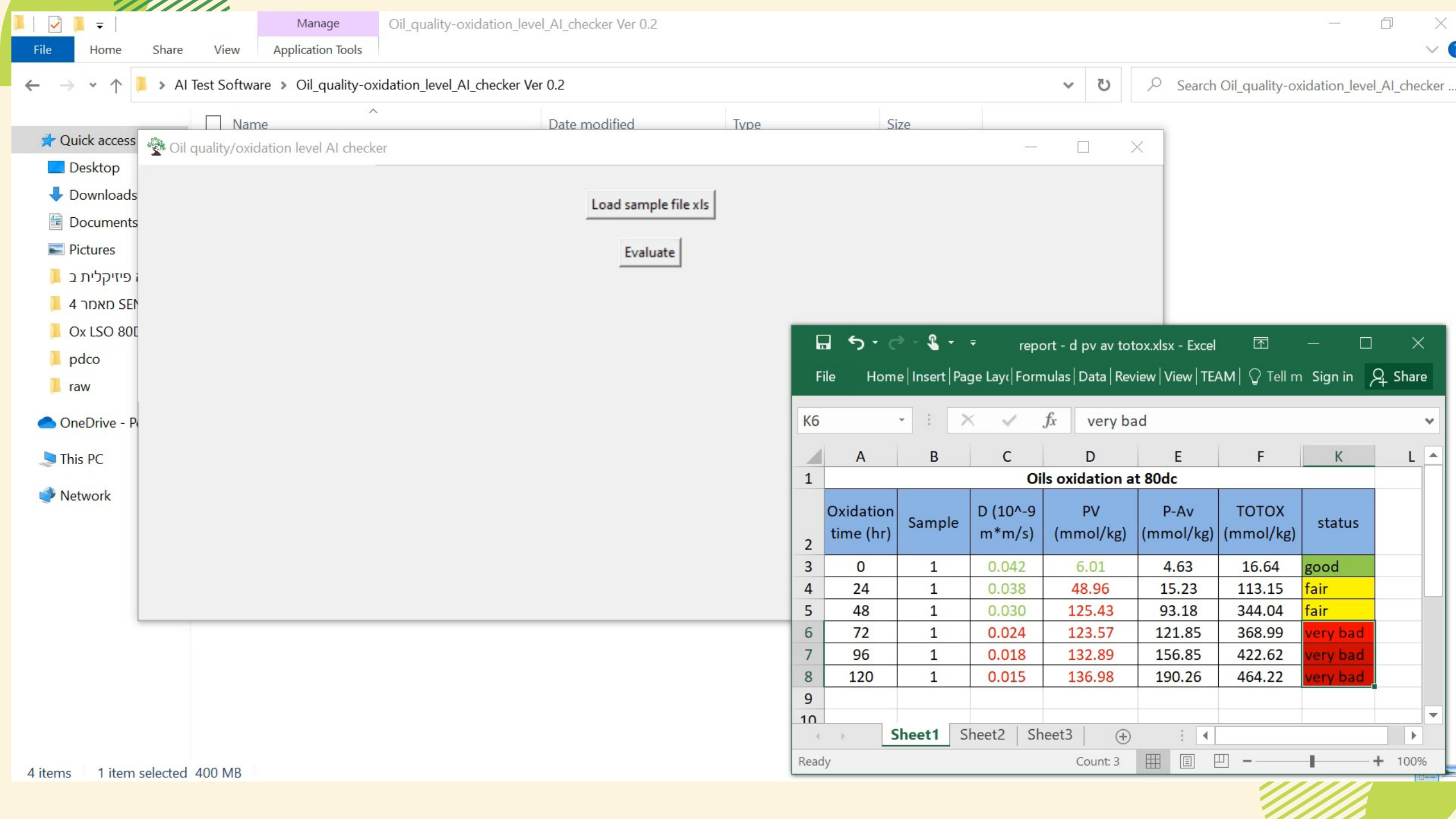
LF NMR T_2 relaxation time of thermal induced linseed oil samples oxidation. Each line color represents from top to bottom T_2 relaxation time (0hr, 12hr, 24hr, 48hr, 96hr, 120hr).





System set up, a typical workflow where a drop of oil is scanned with a LF-NMR machine; in the next step the CNN use the T_2 signal as an input and return the oil oxidation class as output.





Oil quality/oxidation level AI checker

Load sample file xls

Evaluate

report - d pv av totox.xlsx - Excel

File Home Insert Page Layout Formulas Data Review View TEAM Tell me Sign in Share

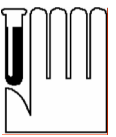
K6 very bad

	A	B	C	D	E	F	K	L	
1	Oils oxidation at 80dc								
2	Oxidation time (hr)	Sample	D (10 ⁻⁹ m*m/s)	PV (mmol/kg)	P-Av (mmol/kg)	TOTOX (mmol/kg)	status		
3	0	1	0.042	6.01	4.63	16.64	good		
4	24	1	0.038	48.96	15.23	113.15	fair		
5	48	1	0.030	125.43	93.18	344.04	fair		
6	72	1	0.024	123.57	121.85	368.99	very bad		
7	96	1	0.018	132.89	156.85	422.62	very bad		
8	120	1	0.015	136.98	190.26	464.22	very bad		
9									
10									

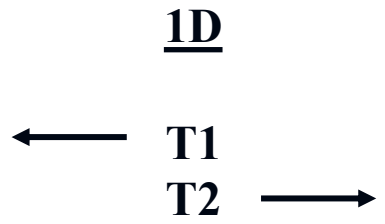
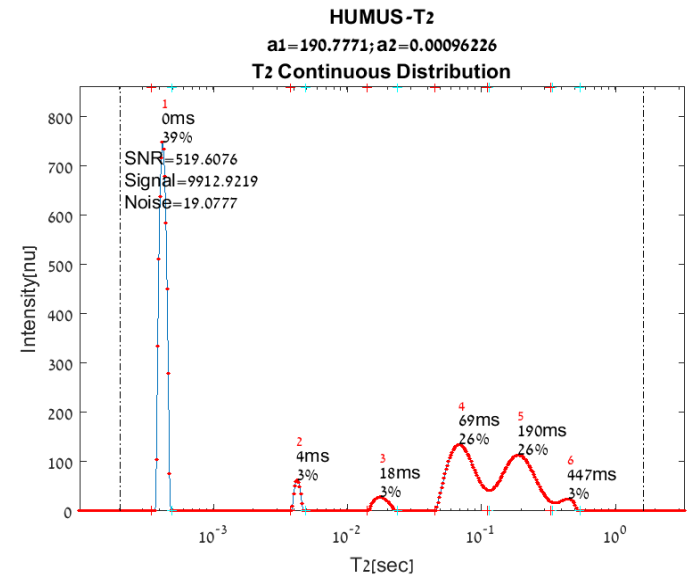
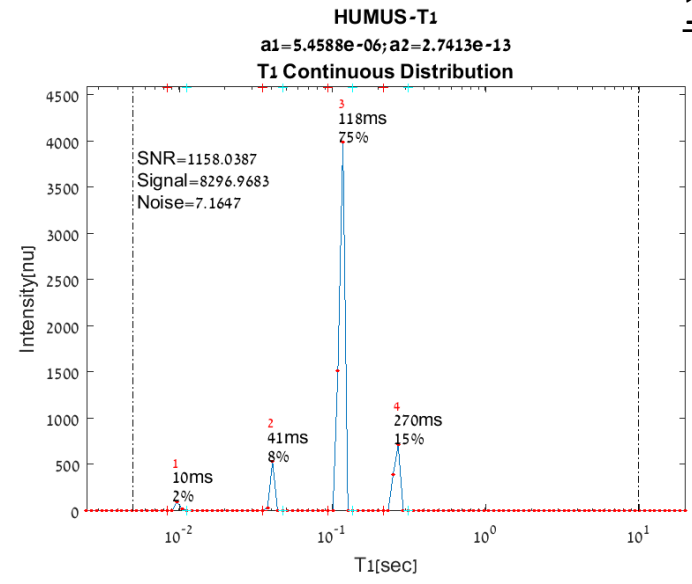
Sheet1 Sheet2 Sheet3

Ready Count: 3 100%

Cicer arietinum seeds (Hummus) TD NMR Sensor Structure Signature

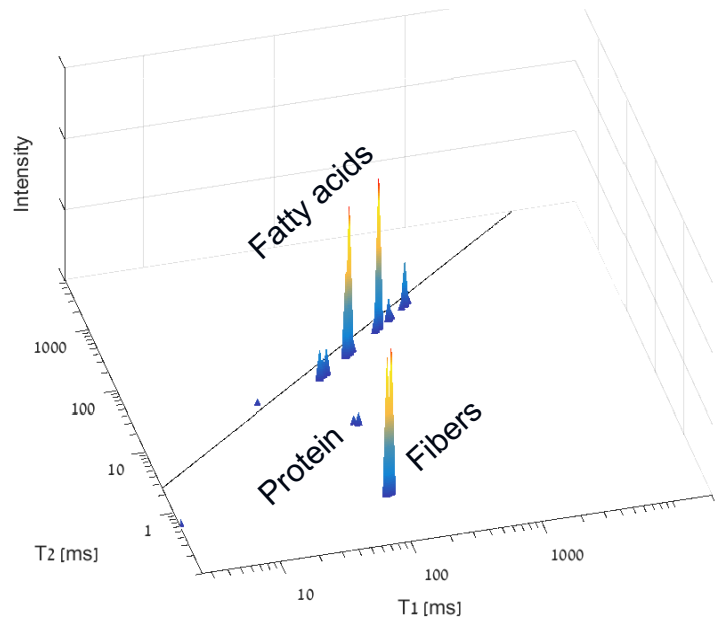


1D Structure Signature



2D Structure Signature

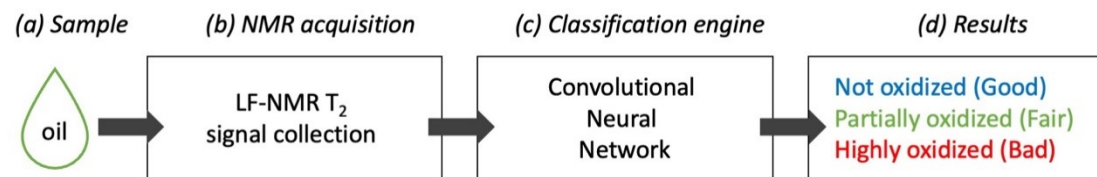
2D T1-T2 →



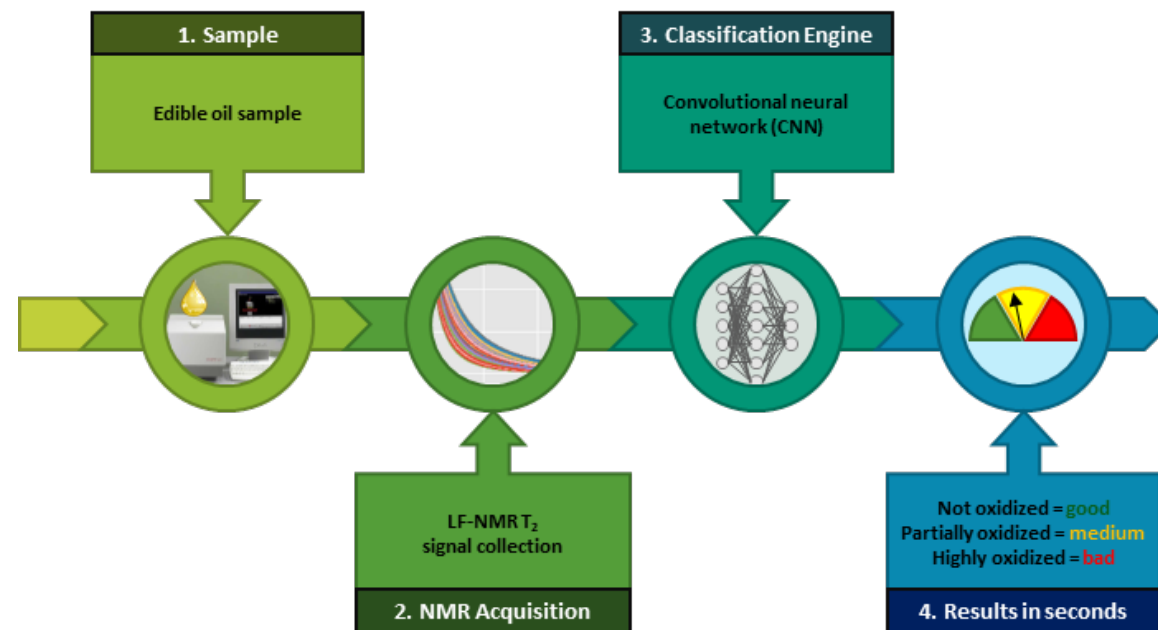
Phase I

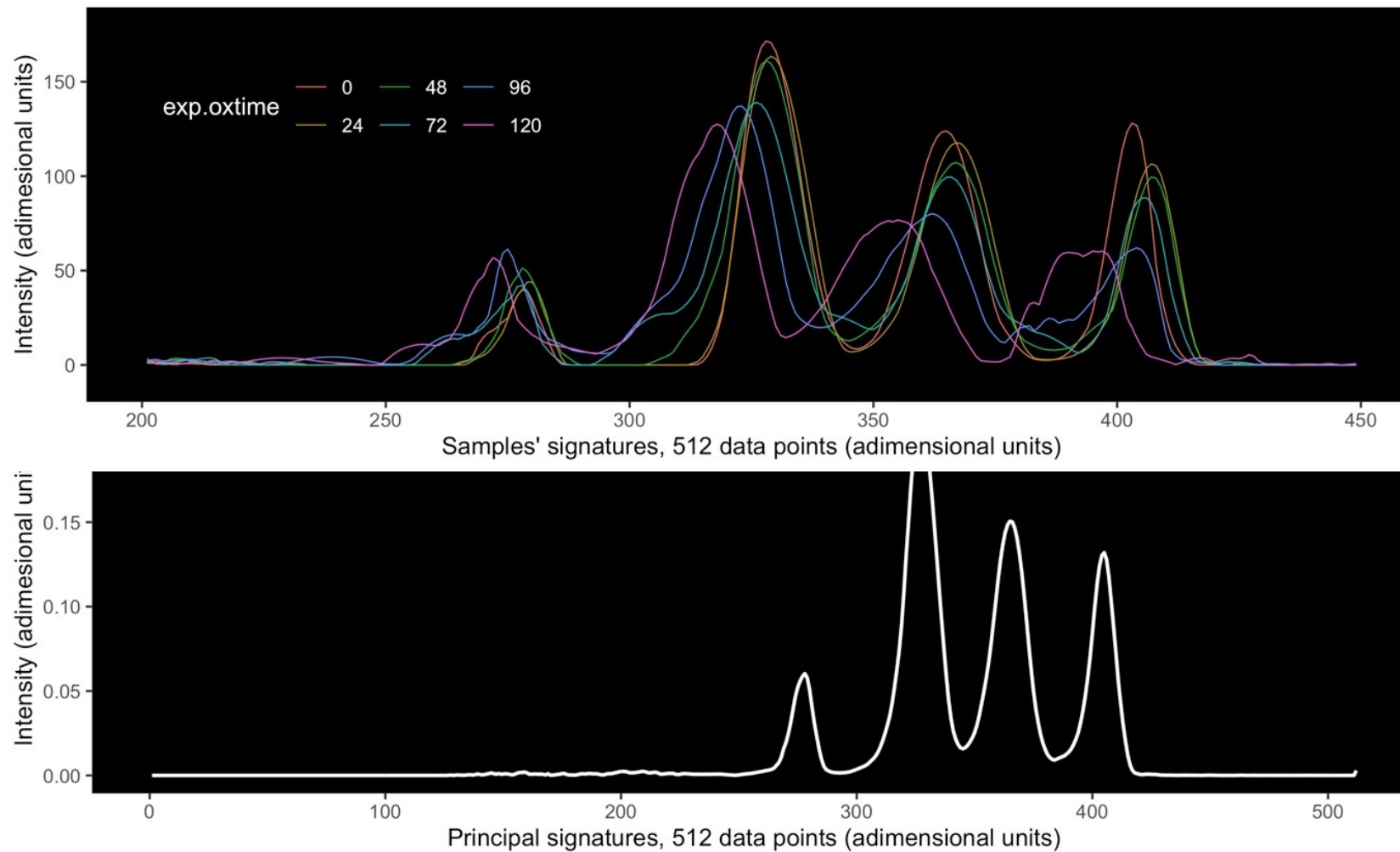
Machine Learning for Oil Safety-Quality classification

based on
Convolutional Neural Networks (CNN)
built on Tensor Flow technology



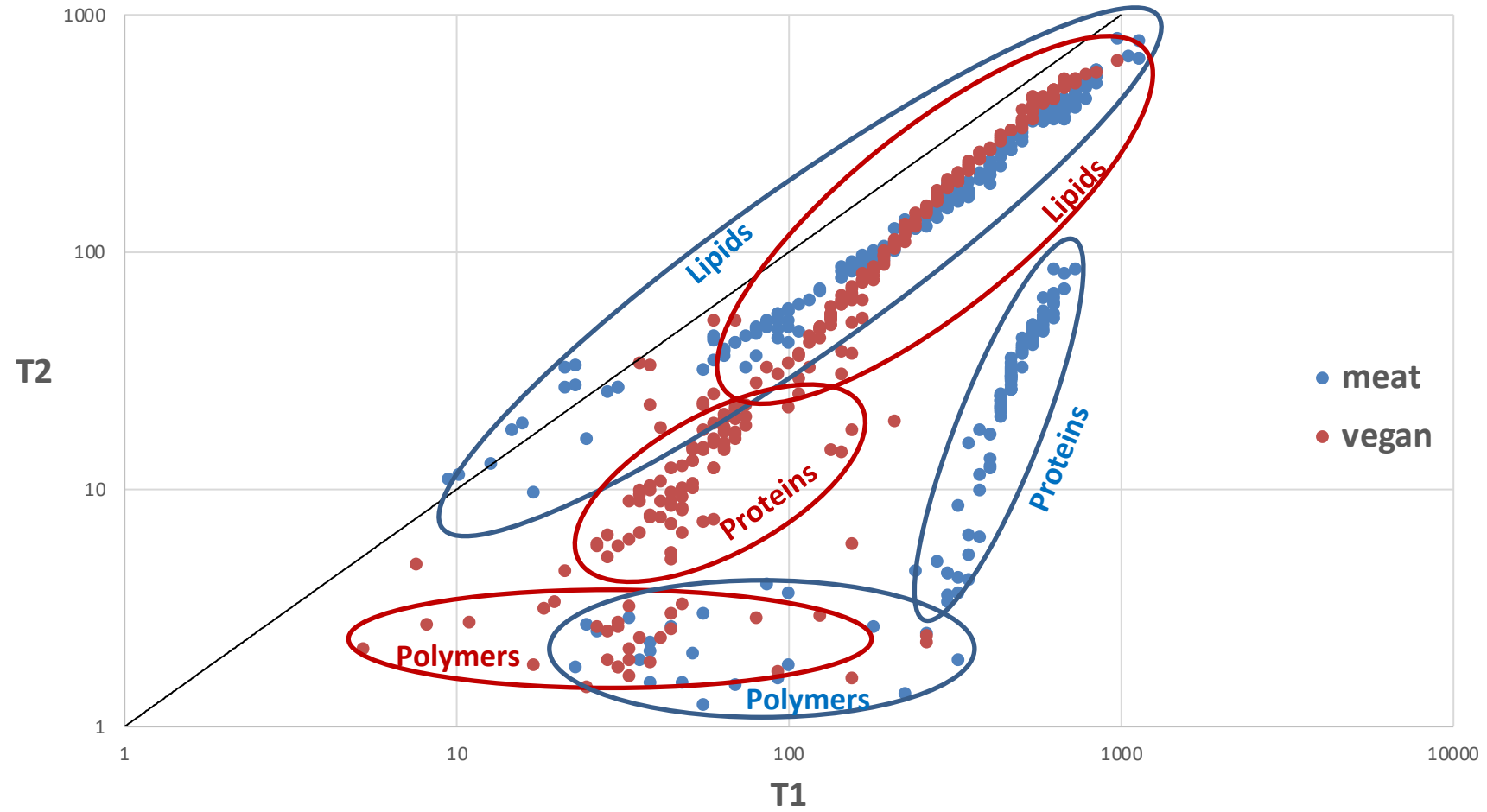
AI NMR Sensor for Edible Oil Oxidation





TD NMR signatures for Linseed oil at different oxidation levels

resulting from different oxidation treatments for the duration of 0, 24, 48, 72, 120 hr. Different oxidation levels in different colors; each signature results from the algebraic summary of various experimental repetitions. Top panel shows the signatures as normally rendered by the NMR machine; Low panel is a synthesis of all Linseed experiments included in the lage database.



NMR T1-T2 chemical and structural MAPPING OF ANIMAL MEAT
AND VEGAN PLANT BASED MEAT SUBSTITUE

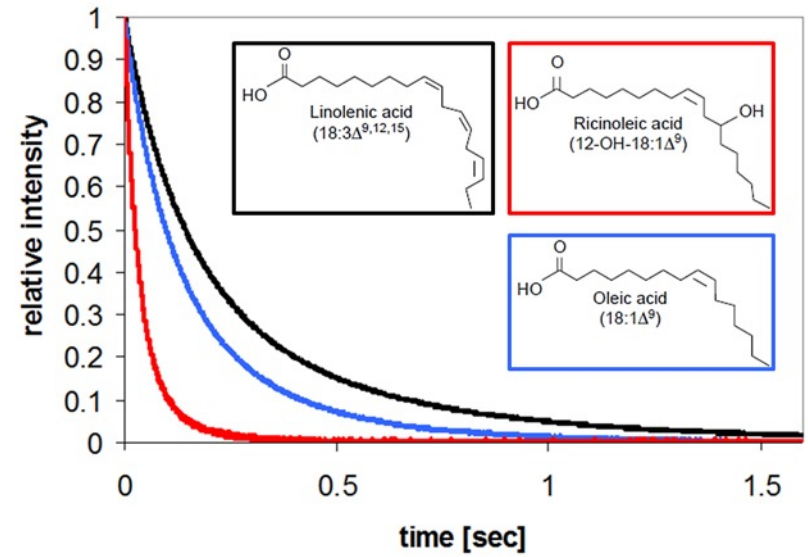
NMR Precision Teslameter
PT2026



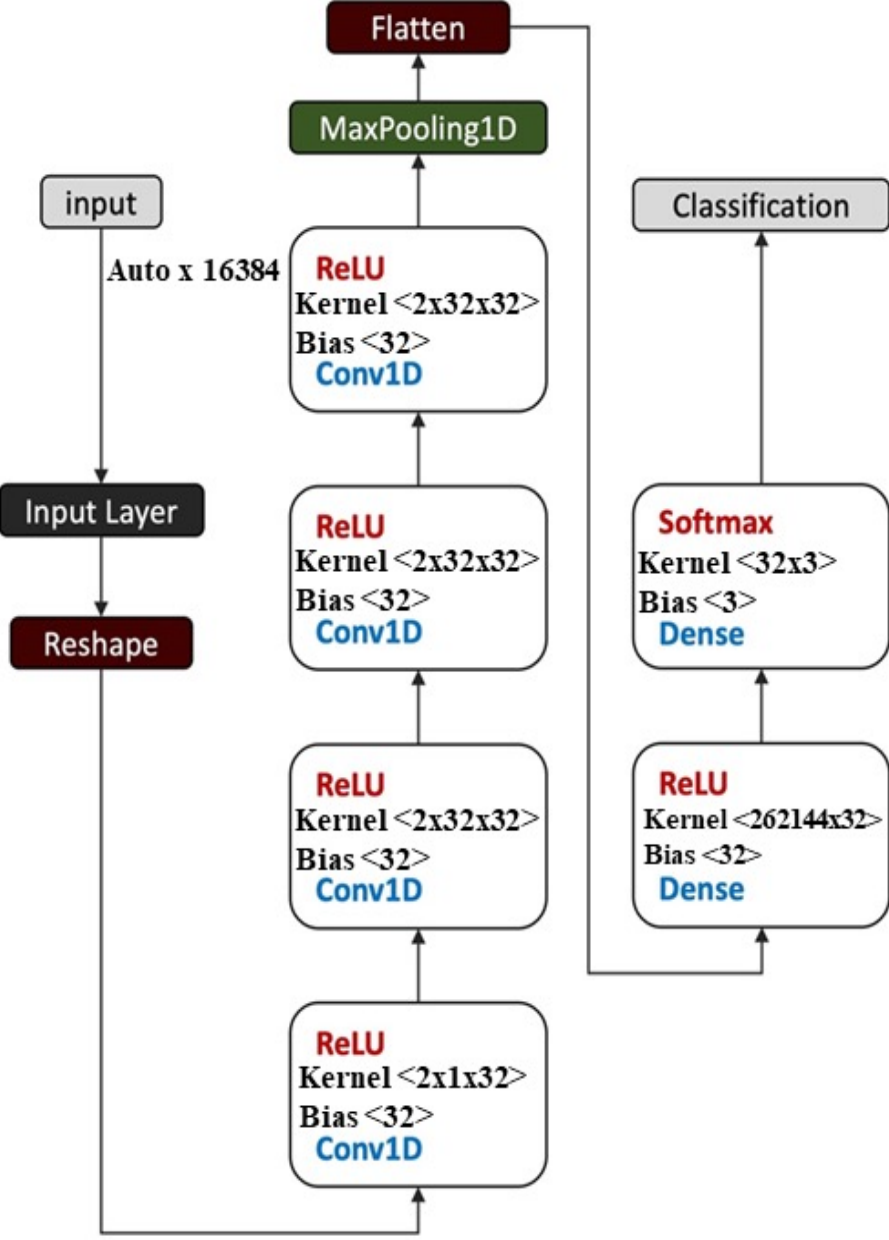
World's most
precise magnetometer

The image shows a white rectangular device (the PT2026 teslameter) connected to a laptop and a probe. The laptop screen displays a software interface with various data plots and graphs. The background is dark blue with some faint icons and text.

- linseed
- olive
- castor



Convolutional neural network (CNN) architecture including input layer, convolution layers, pooling layer, output layer, and classification (Conv1D = Conversion 1D).





2022 IBM - AI for Quality Test





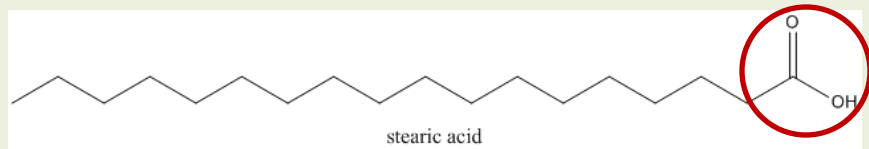
Intelligent LF-NMR Sensor in the field of Biodiesel



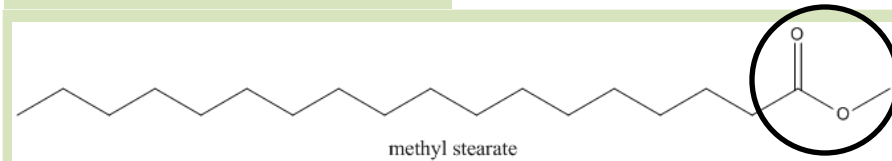


Chemical structure of representative common FAs and FAMES

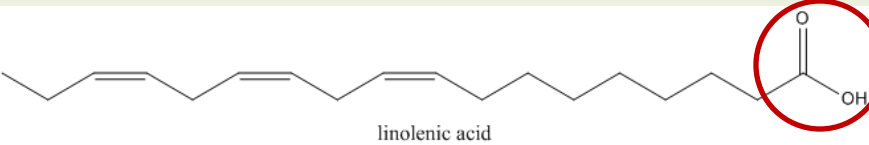
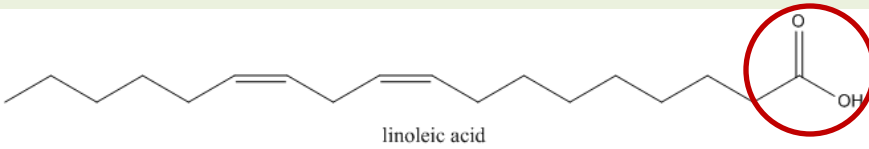
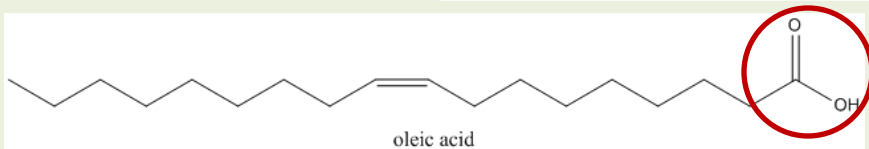
Saturated FAs



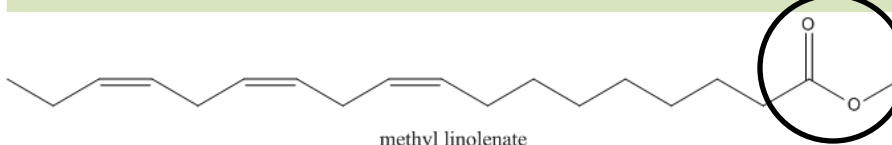
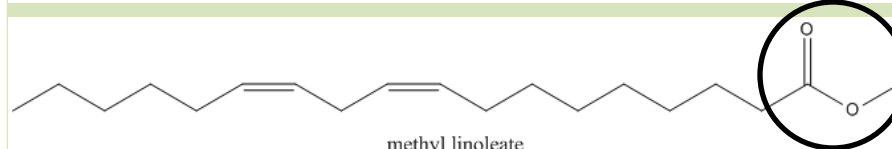
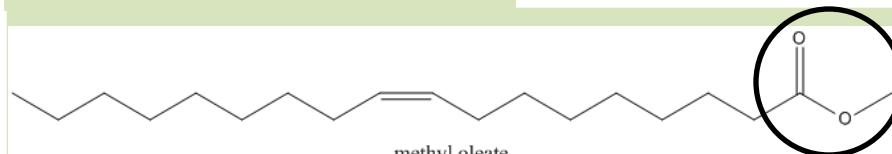
Saturated FAMES



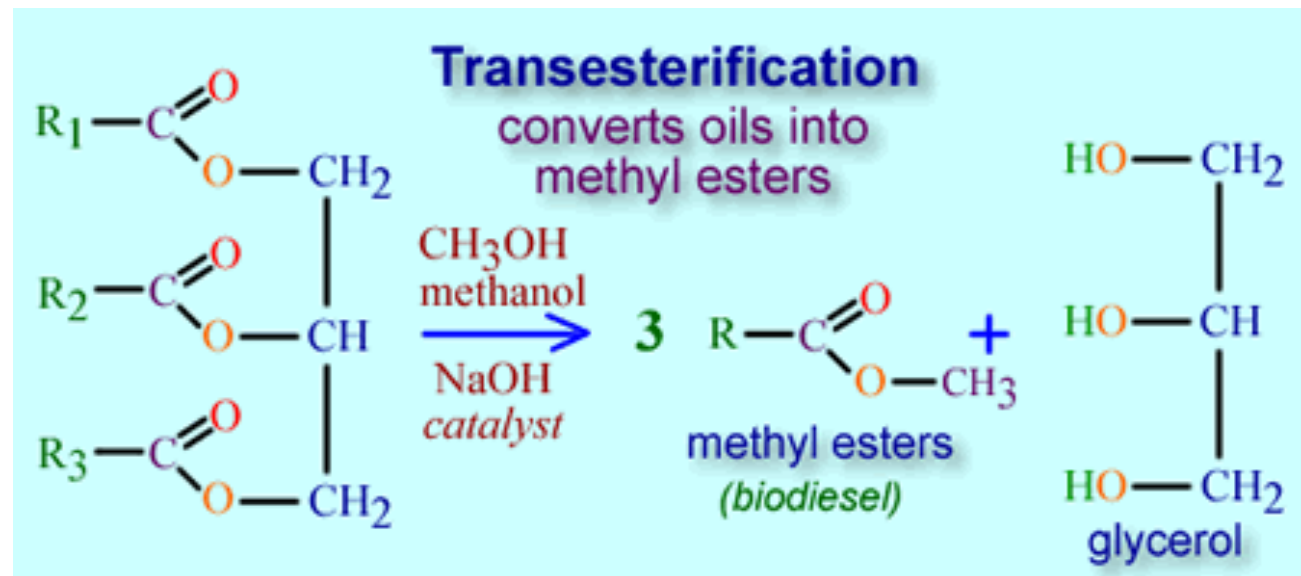
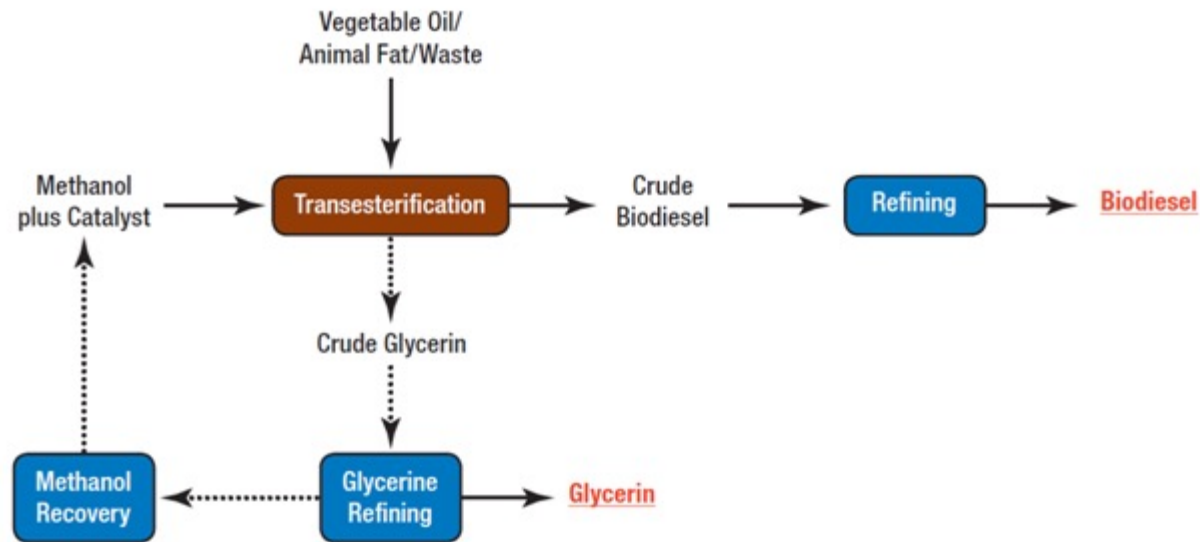
Unsaturated FAs



Unsaturated FAMES



Schematic of Biodiesel Production Path

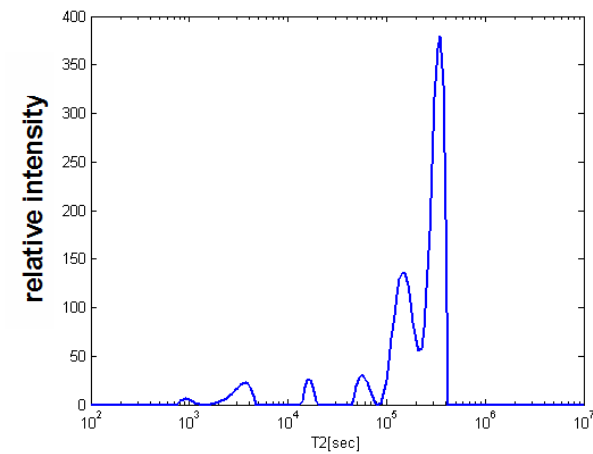
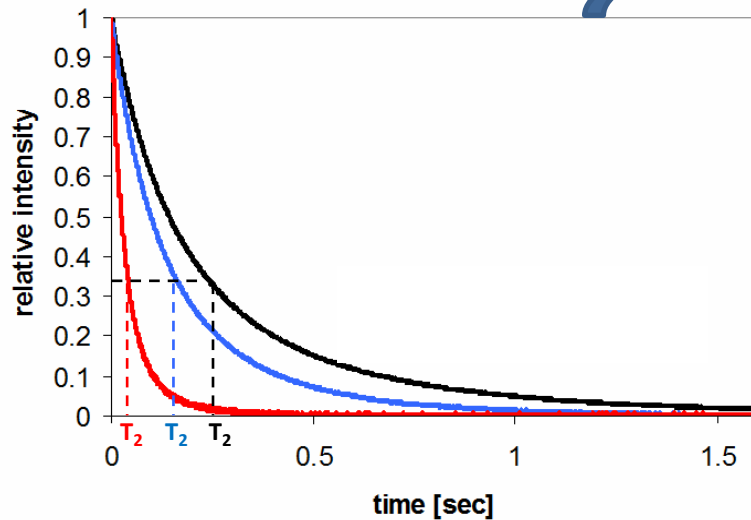




CPMG Pulse Sequence – T_2

Inverse Laplace Transform

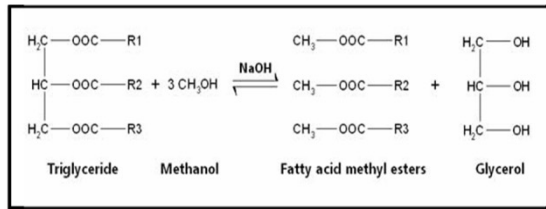
$$M(t) = \int F(T_2) \exp(-t/T_2) dT_2$$



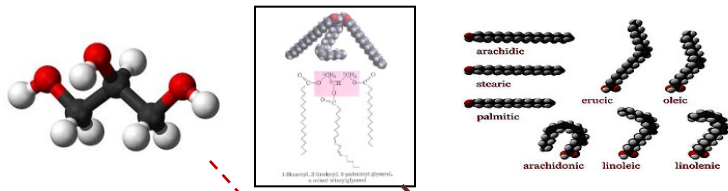
Demonstration of T₂ Relaxation of FAMES in LF-NMR



Transesterification

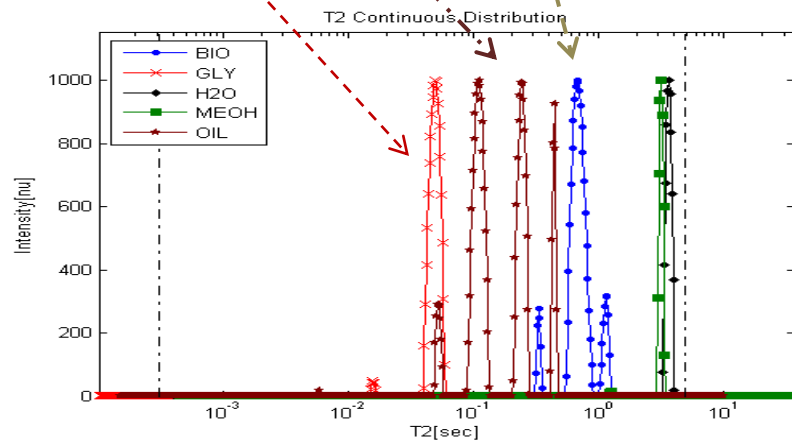
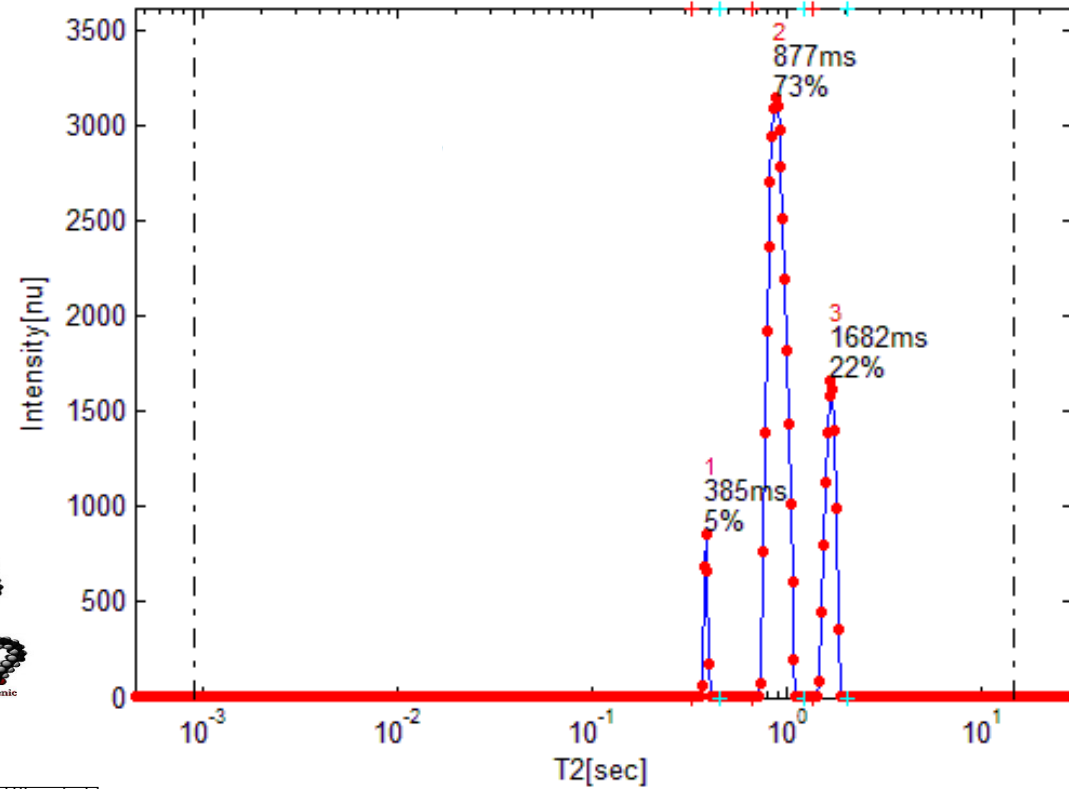


Monitoring of Biodiesel Process



Linseed-Biodiesel

T₂ Continuous Distribution



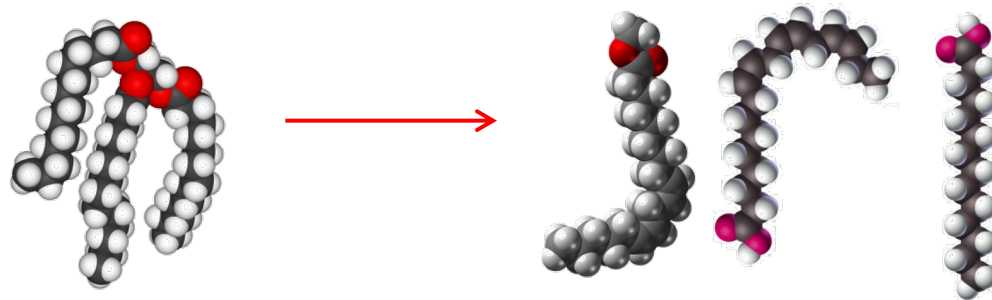
Mobility – Fluidity →

← Viscosity

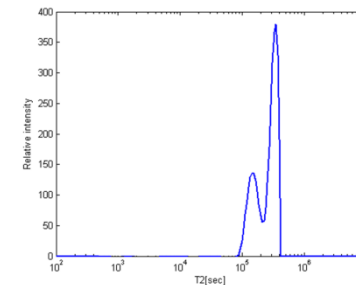


Additional Relevant Background

- ^1H LF-NMR spin-spin (T_2) relaxometry can be applied to differentiate between populations in complex systems.
- Triacylglycerols (TAGs) are the most common biodiesel source. They create FAMES in a transesterification reaction:

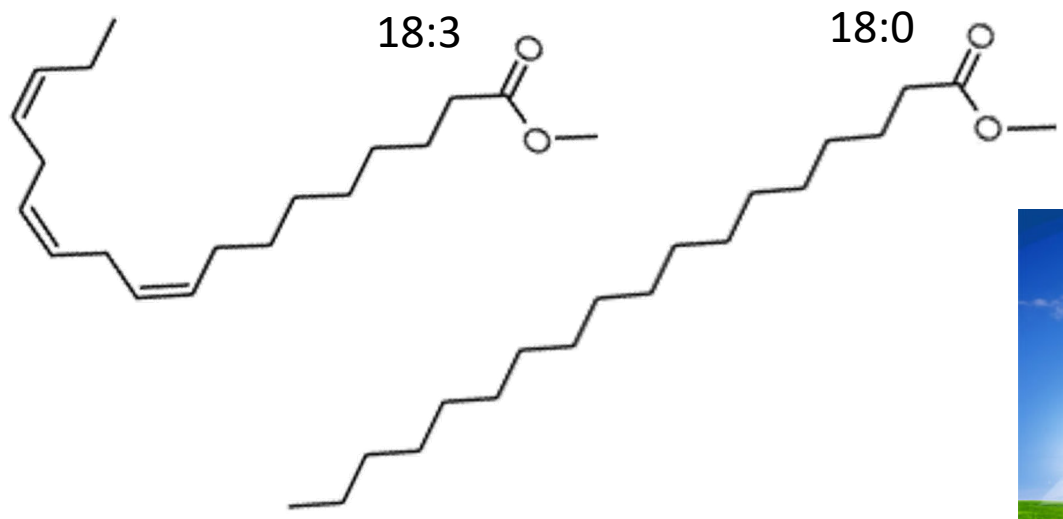


- The analyzed T_2 distribution of TAGs is a bimodal distribution, but there isn't a certainty about the origin of the peaks. 2 hypotheses:
 - inhomogeneous relaxation rates for the protons along the side chains,
 - or
 - inhomogeneous organization of TAGs in the liquid with intermolecular interactions.





- The physical properties of biodiesel are determined by the **length of the hydrocarbon chain**, the **degree of unsaturation**, and the effect of **molecular packing**.
- The liquid structure of FAMES affects the physicochemical properties of the biodiesel including viscosity, density, fluid dynamics and low temperature operability. These properties are of high importance to the field of biodiesel.



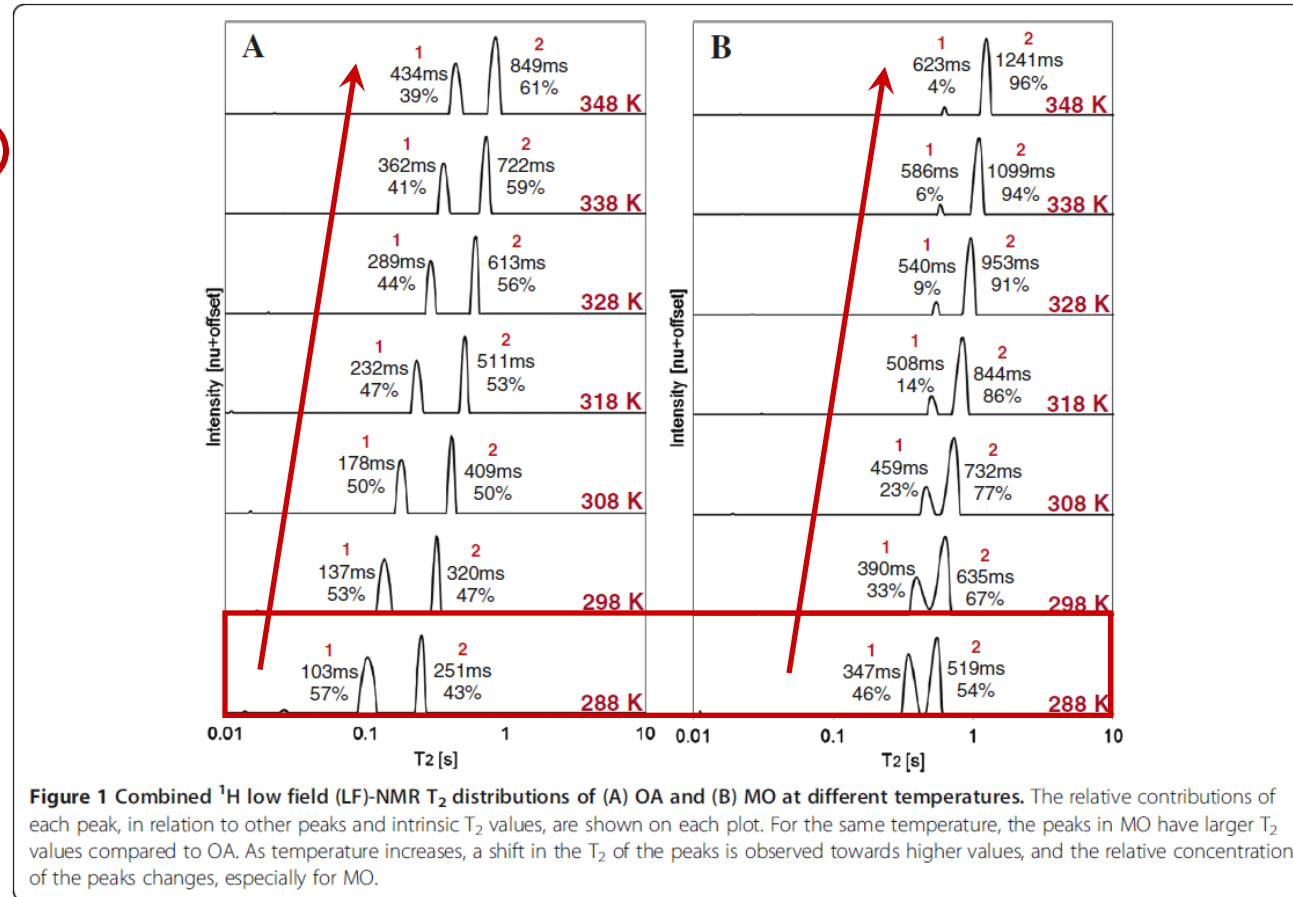
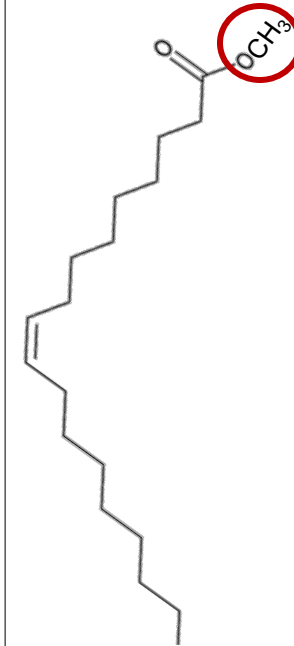
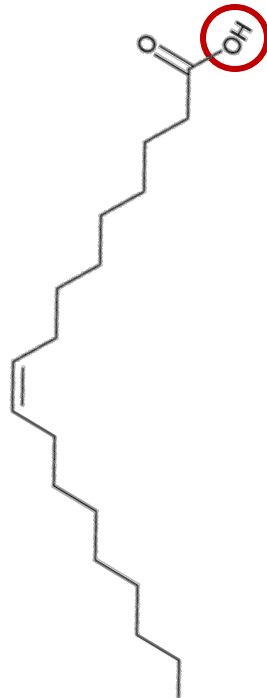


Figure 1 Combined ^1H low field (LF)-NMR T_2 distributions of (A) OA and (B) MO at different temperatures. The relative contributions of each peak, in relation to other peaks and intrinsic T_2 values, are shown on each plot. For the same temperature, the peaks in MO have larger T_2 values compared to OA. As temperature increases, a shift in the T_2 of the peaks is observed towards higher values, and the relative concentration of the peaks changes, especially for MO.

These differences are attributed to a **methyl ester** versus a **carboxylic head group**, which are responsible for the **intermolecular interactions** of one chain with its neighbor.

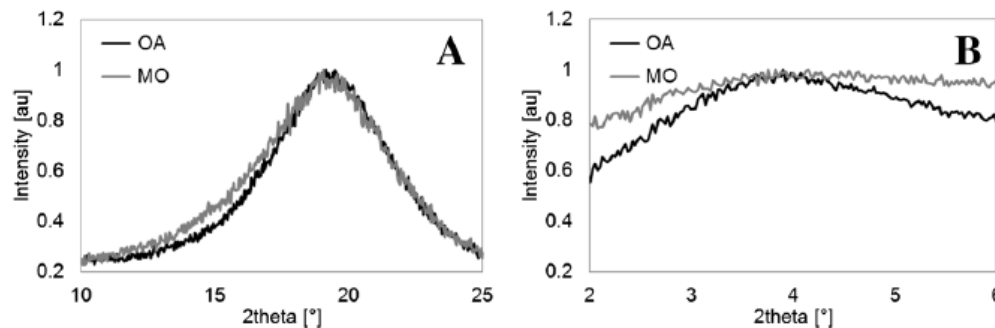
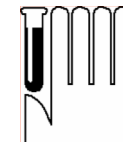


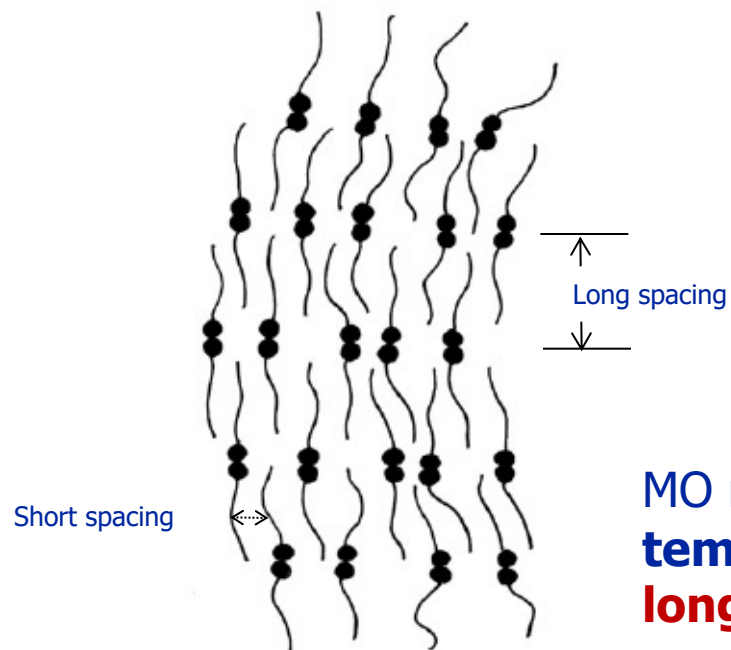
Figure 4 X-ray spectra of OA and MO measured using (A) XRD and (B) SAXS at 298 K. The peak at around 0.14 nm^{-1} ($2\theta \approx 19.8^\circ$) is sharp for both materials, whereas the peak at around 0.03 nm^{-1} ($2\theta = 4.2^\circ$) is very broad and difficult to resolve, especially for the MO sample. SAXS: small angle X-ray scattering; XRD: X-ray diffraction.

Table 1 Short- and long-range spacing, d , of OA and MO at 298 K

	d_{OA} [nm]	d_{MO} [nm]
Short spacing (XRD)	0.459	0.460
Long spacing (SAXS)	2.383	2.531
		2.517 ^a

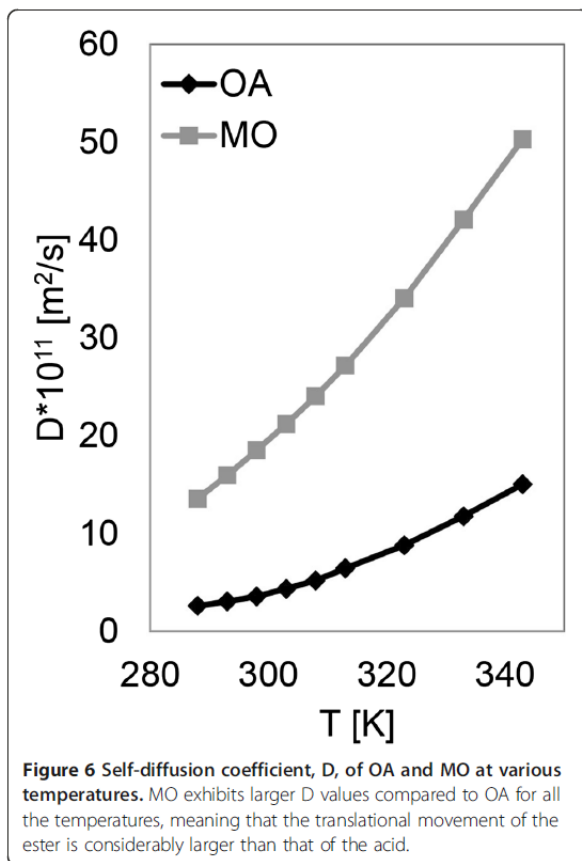
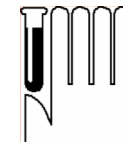
^aLong spacing measured at 263 K.

d_{OA} and d_{MO} are the short- and long-range spacings of OA and MO, respectively. SAXS: small angle X-ray scattering; XRD: X-ray diffraction.



MO molecules have a **larger fluidity**, because as the **temperature is increased**, MO molecules separate both **longitudinally and transversely** from one another.

Translational motion through ^1H LF-NMR diffusometry



Both materials exhibit Arrhenius dependence of the form:

$$D = D_0 \exp(-\Delta E_{app} / RT)$$

with apparent activation energies, ΔE_{app} , of **27.0** and **19.5** KJ/mol for the OA and MO molecules, respectively.

Table 2 Dynamic viscosity, η , of MO and apparent hydrodynamic radius, r , of MO and OA according to temperature

T [K]	η_{MO} [mPa s]	r_{MO} [nm]	r_{OA}^a [nm]
288	6.97	0.339	
293	6.03	0.332	0.315
298	5.27	0.336	
303	4.66	0.339	0.337
308	4.14	0.340	
313	3.71	0.341	0.330
318	3.34		
323	3.03	0.344	0.337
328	2.76		
333	2.52	0.345	0.345
338	2.32		
343	2.15	0.348	0.364
348	1.99		
353	1.85		
358	1.72		

^aCalculated using the dynamic viscosities given in [19]. η_{MO} is the dynamic viscosity of MO; r_{MO} and r_{OA} are the apparent hydrodynamic radii of MO and OA, respectively.

η measurements were used to calculate r from the Stokes-Einstein formula under a slip boundary condition.

$$r = \frac{kT}{4\pi\eta D}$$

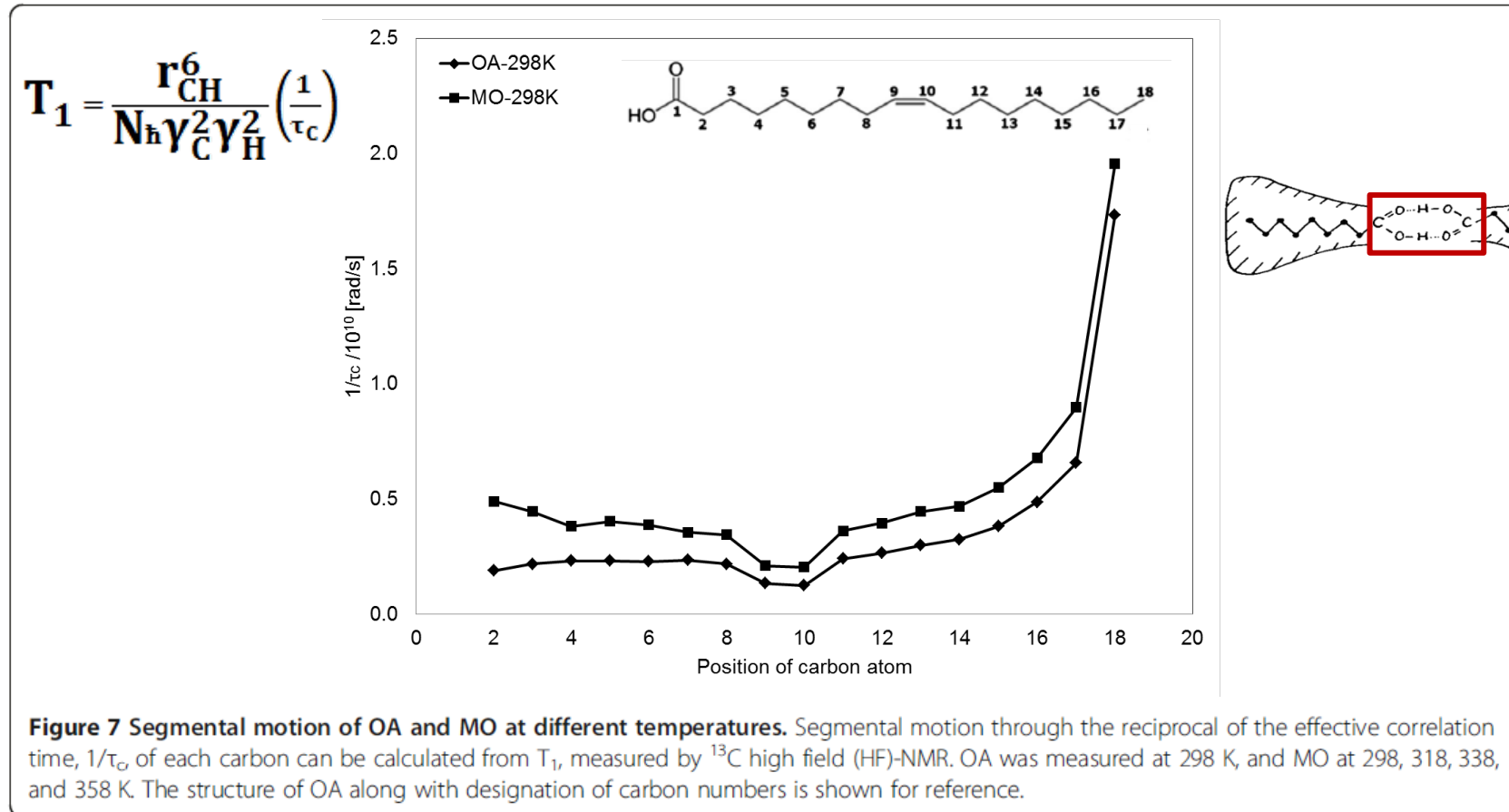
The motion for long rod-like molecules is restricted to **linear molecular movement**; therefore, similar r values for the OA and MO molecules are to be expected.



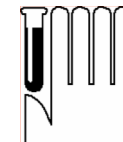
Rotational (segmental) motion through ^{13}C HF-NMR relaxometry



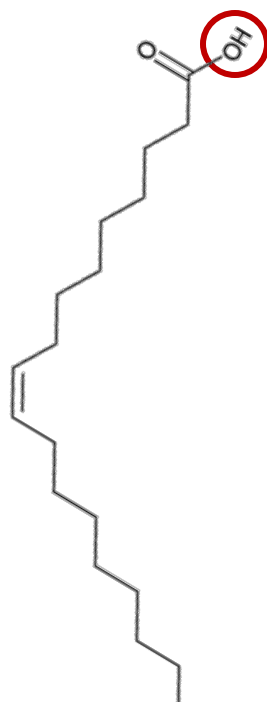
The **correlation time** is the average time it takes for a molecule to progress through **one radian** via random molecular tumbling (**Brownian motion**).



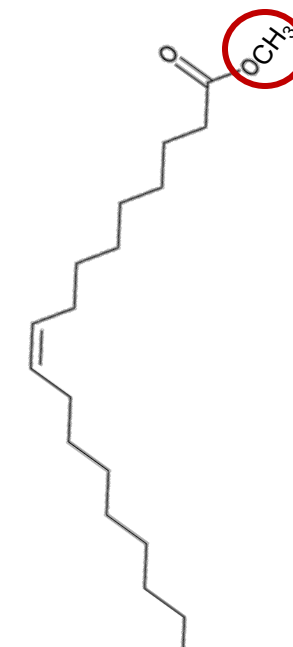
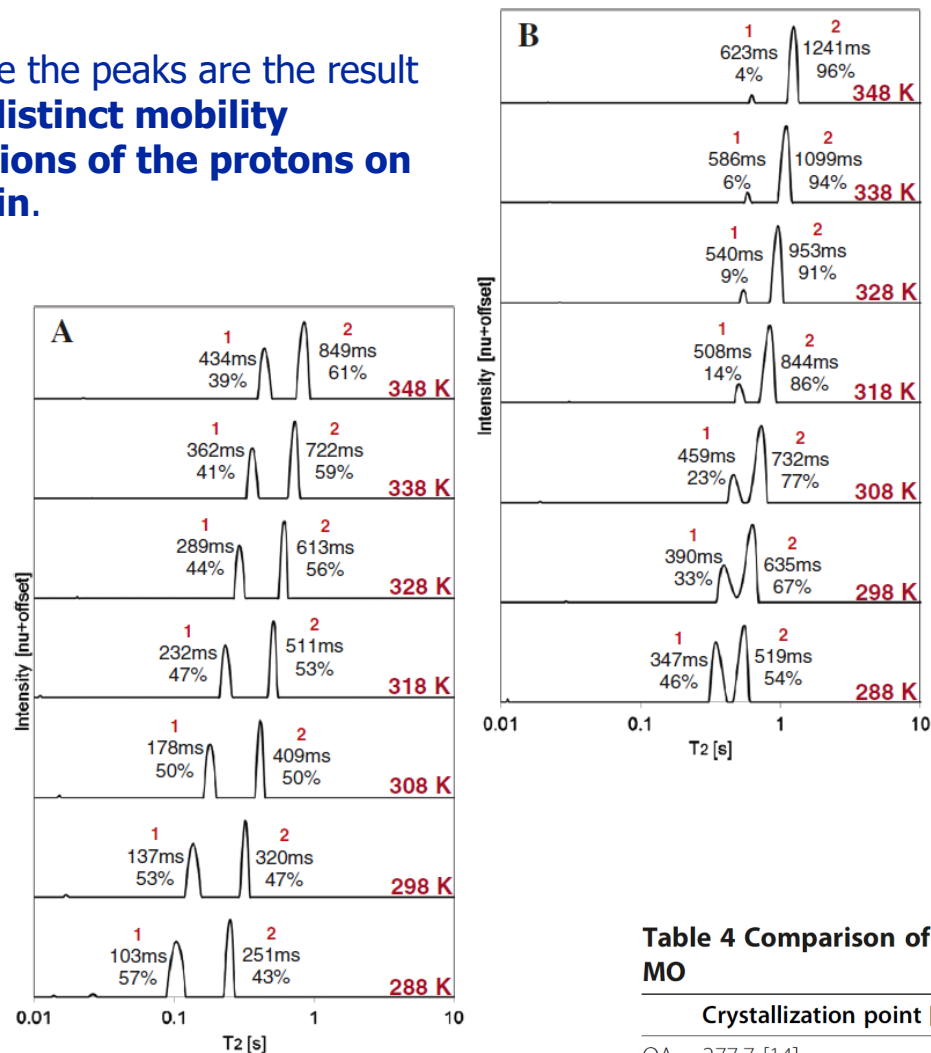
Translational diffusion is probably initiated by the **ends of the molecules**. In the case of OA, dimers of two hydrogen-bonded molecules would move by the flipping of both tails on the dimer. MO molecules, on the other hand, would find available spaces for translational movement by very vigorous rotation of the tail, but also by wagging of the head.



^1H LF-NMR T_2 distributions at different temperatures



Therefore the peaks are the result of **two distinct mobility populations of the protons on the chain**.



The response of the peaks with temperature suggests an **increase in the mobility of different protons along the chain**, or a **change in the molecular organization** towards the higher mobility peak.

Table 4 Comparison of phase transition points of OA and MO

	Crystallization point [K]	Melting point [K]	Boiling point ^a [K]
OA	277.7 [14]	286.0 ^b [14]	496.0 [42]
MO	232.5 [43]	253.1 [35]	474.0 [42]

^aMeasured at 1.333 kPa.

^bThe melting point for the α polymorph is referenced.



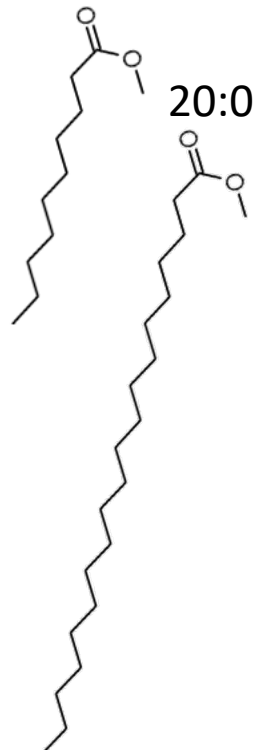
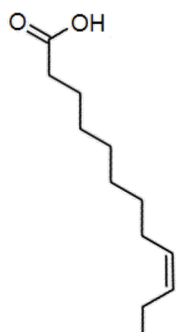
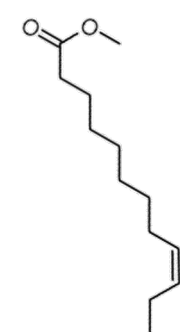
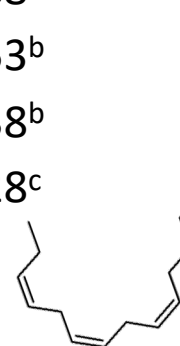
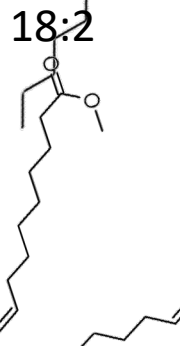

Bearing in mind that the **mobility of the molecules** is the direct outcome of their **morphological structure**, the differences in the molecular arrangement of OA and MO can be proposed by monitoring the differences in T_2 distributions and peak area in response to a gradient of temperatures.

This can be observed from the similarities in T_2 distributions in relation to melting point. In this way, the large change in relative contribution of the peaks for MO suggests a **less dense packing** compared to OA and a **reduction in intermolecular interactions**.



Chain/tail Length and Unsaturation effect on FAME Packing

Table 1. Melting points used for the materials. T_m s are within ± 2 K from the melting temperatures reported in the literature.

	Common name	Chain type	T_m [K]			
	Methyl caprate	10:0	258 ^a			
	Methyl laurate	12:0	278 ^b			
	Methyl myristate	14:0	293 ^c			
	Methyl palmitate	16:0	303 ^c			
	Methyl stearate	18:0	313 ^c			
	Methyl arachidate	20:0	318 ^d			
	Methyl palmitoleate	16:1	238 ^a			
	Oleic acid	18:1 Acid	288 ^a			
	Methyl oleate	18:1	253 ^b			
	Methyl linoleate	18:2	238 ^b			
Methyl linolenate	18:3	228 ^c				

^a(Knothe & Dunn, 2009)

^b(Knothe, 2005a)

^c(*Handbook of chemistry and physics*2007)

^d(*The lipid handbook*2007)



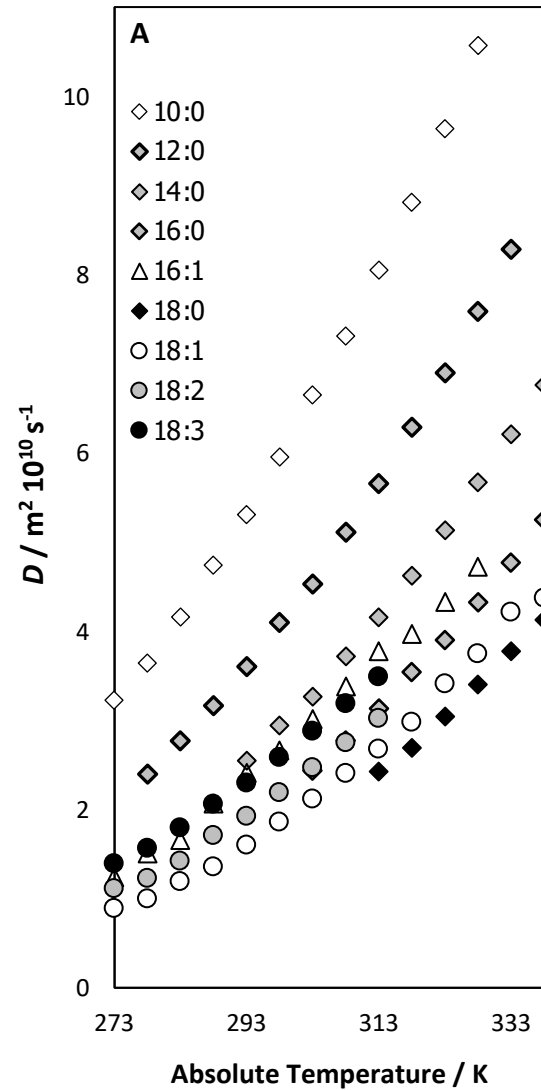
Results: X-Ray

Short- and long-range spacing of 18 carbons chains and saturated FAMEs.

18 carbons chain at 298 K	Short spacing [nm]	Long spacing [nm]
18:1 Acid	0.459	2.383
18:1	0.460	2.531

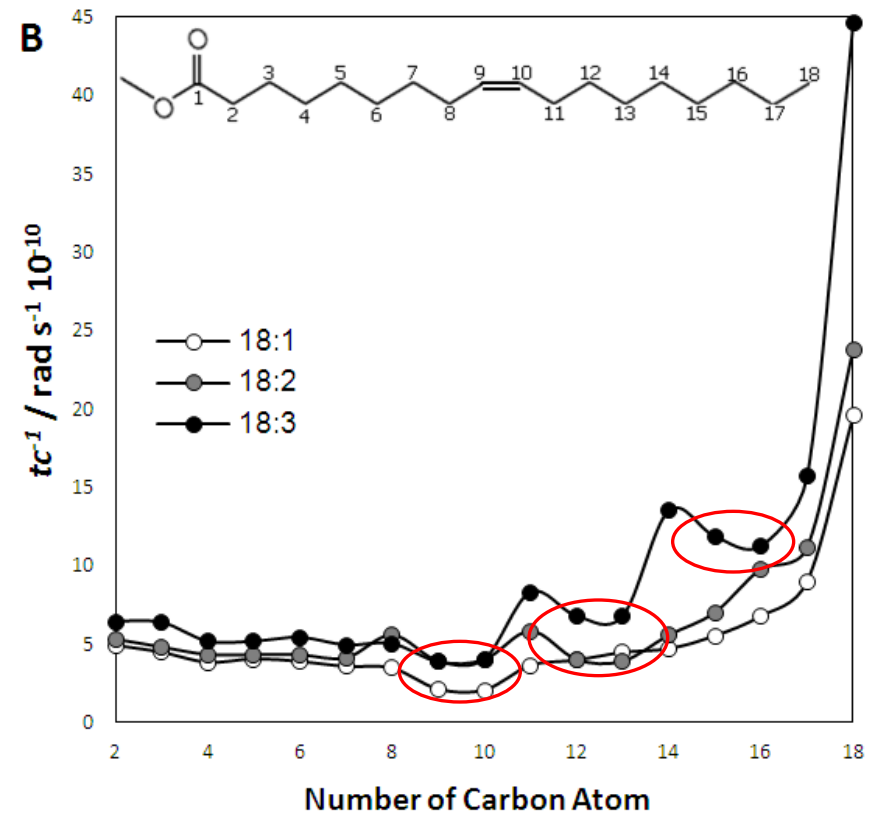
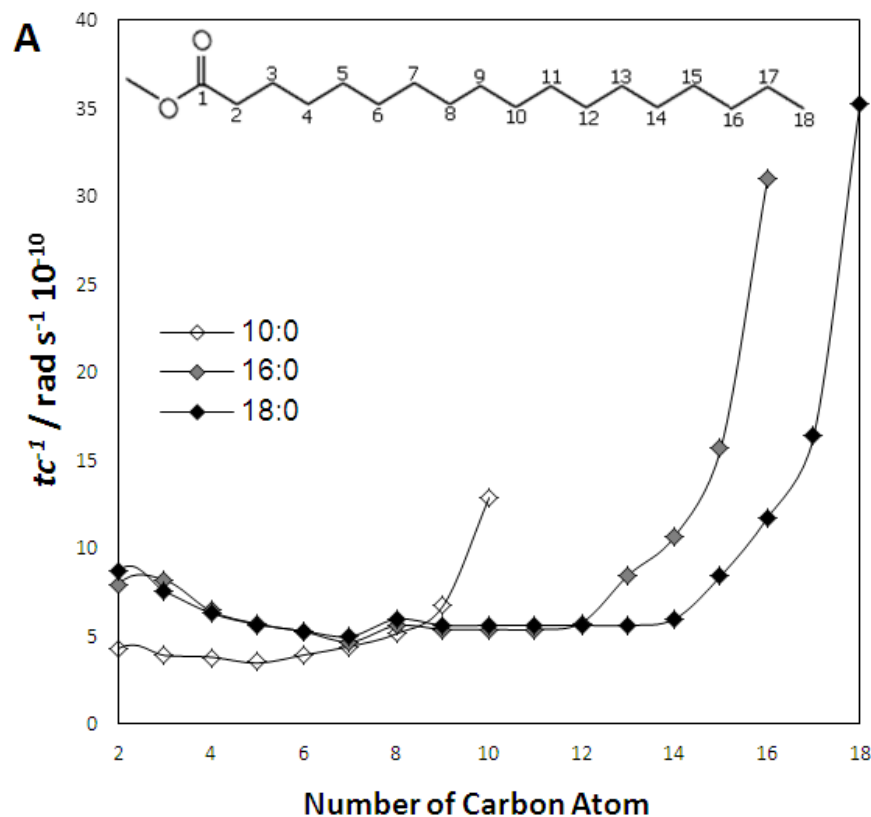
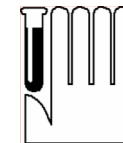


Results: ^1H LF-NMR relaxometry

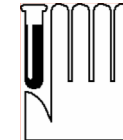


Self-diffusion coefficient, D , versus (A) absolute and (B) specific temperature distances from T_m .

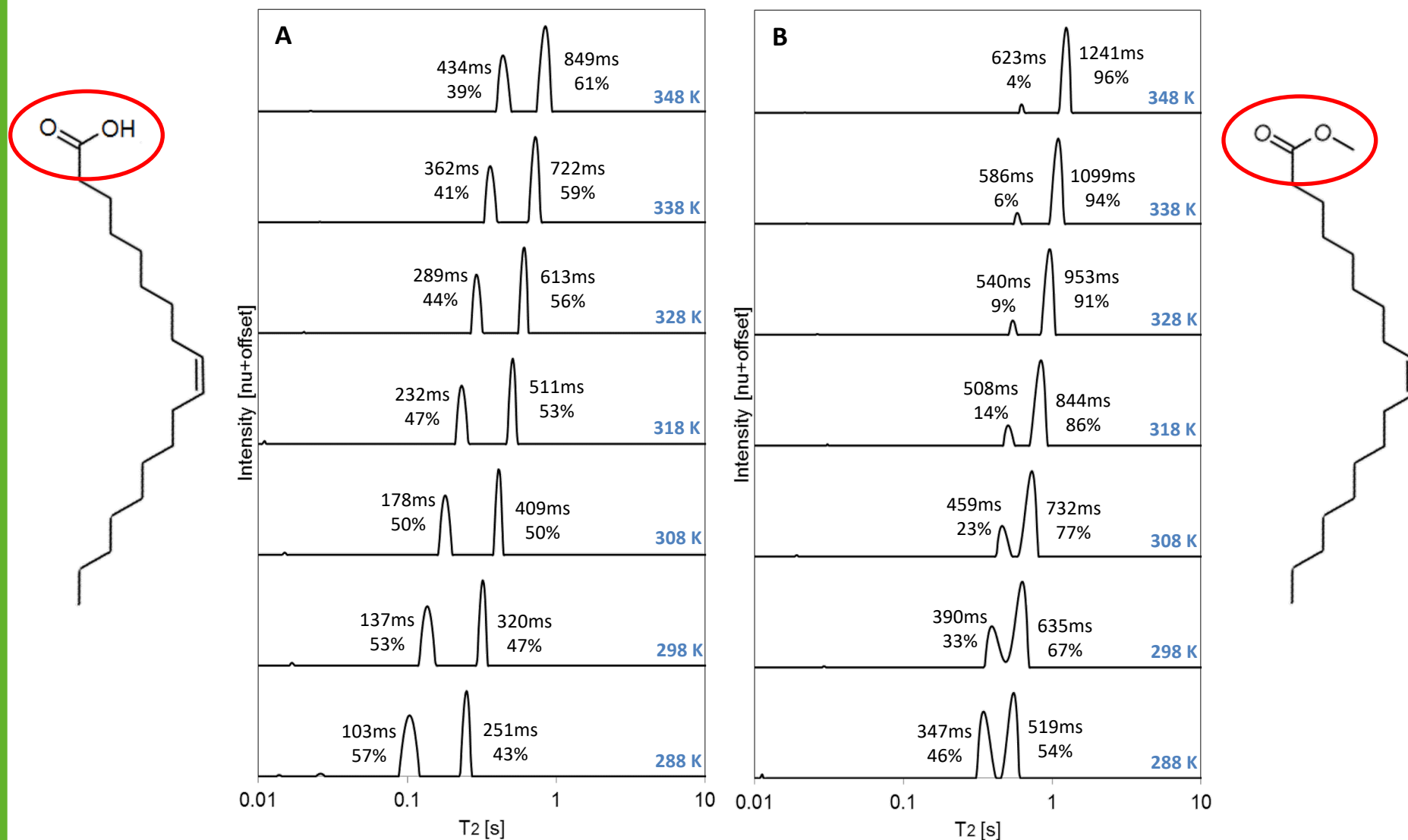
Results: ^{13}C HF-NMR relaxometry



Segmental motion (τ_c^{-1}) of the carbon atoms at different positions of (A) saturated FAMES (10:0, 16:0 and 18:0) at $T_m + 15$ K and (B) unsaturated FAMES (18:1, 18:2 and 18:3) at 298 K.

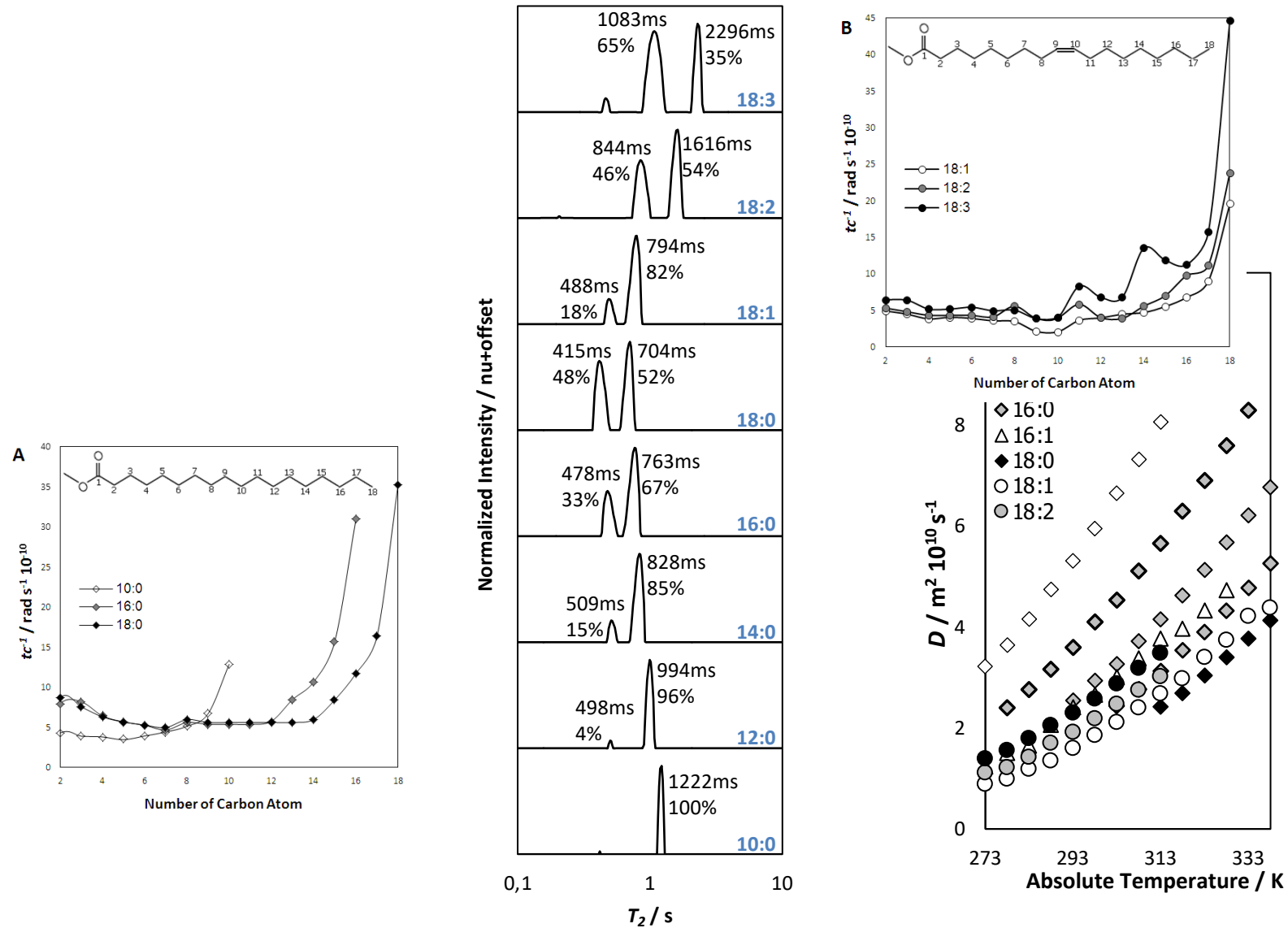


Results: ^1H LF-NMR relaxometry



Combined ^1H LF-NMR T_2 distributions of (A) 18:1 Acid and (B) 18:1 at different temperatures.

Results: ^1H LF-NMR relaxometry



Combined ^1H LF-NMR T_2 distributions of FAMEs at 313 K.



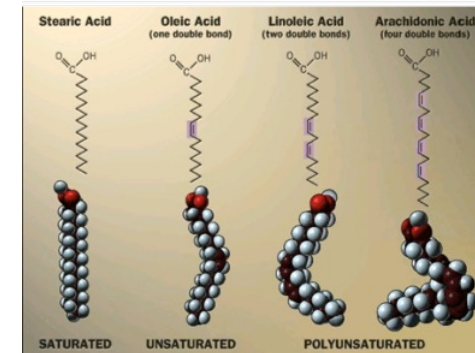
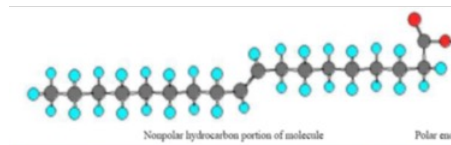
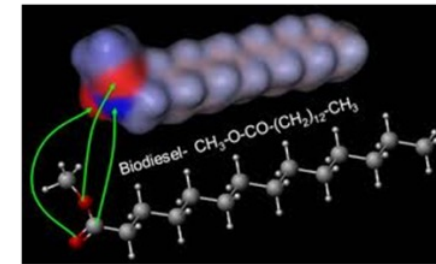
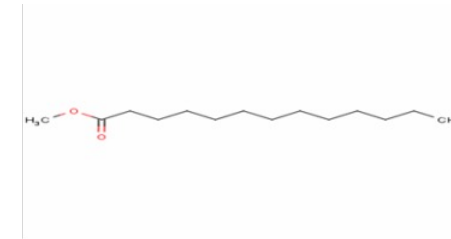
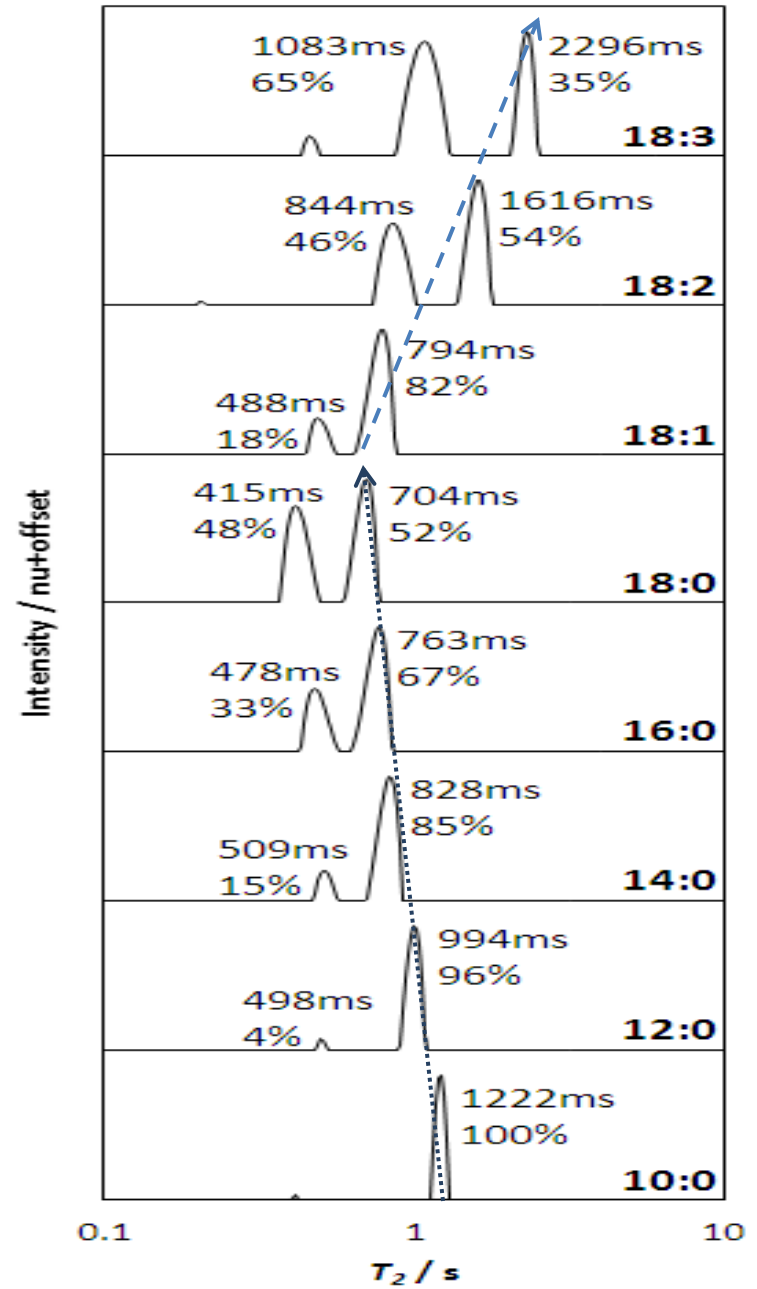
Conclusions

- Both the peaks assignment for ^1H LF-NMR T_2 distributions of FAMEs and the model for their liquid crystal-like arrangement in the liquid phase were confirmed.
- NMR and especially LF-NMR relaxometry would be an excellent tool for monitoring changes in molecular packing and/or weak interactions of fatty acids and FAMEs.
- This new application is of high prospective to the field of biodiesel, and to other research and applied disciplines with the potential of studying numerous physicochemical- and organizational-based properties, processes and mechanisms of alkyl chains.

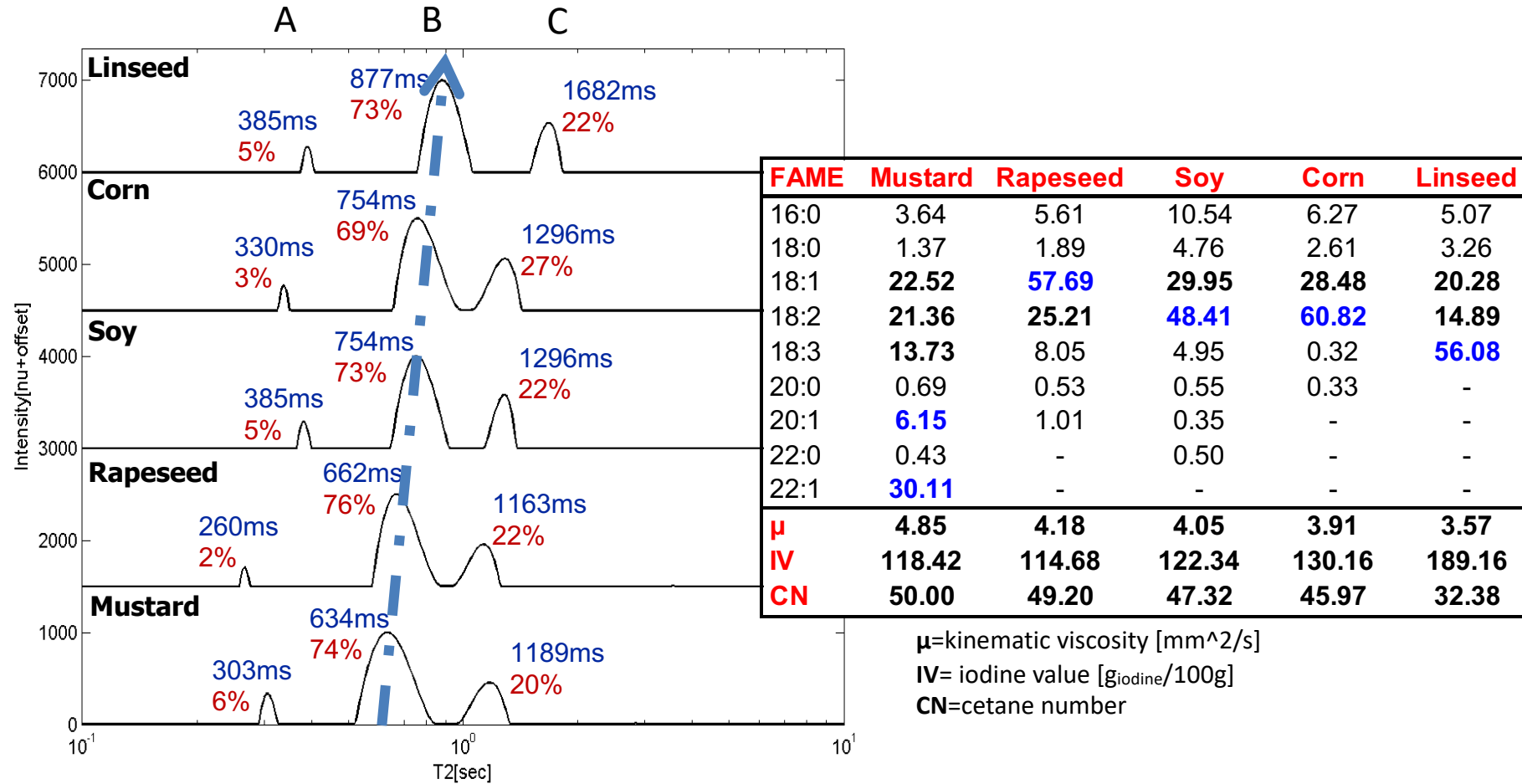




T₂ relaxation times of saturated & unsaturated FAMES at 40°C



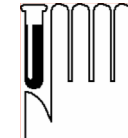
T₂ of Bio FAME Mix at 40°C



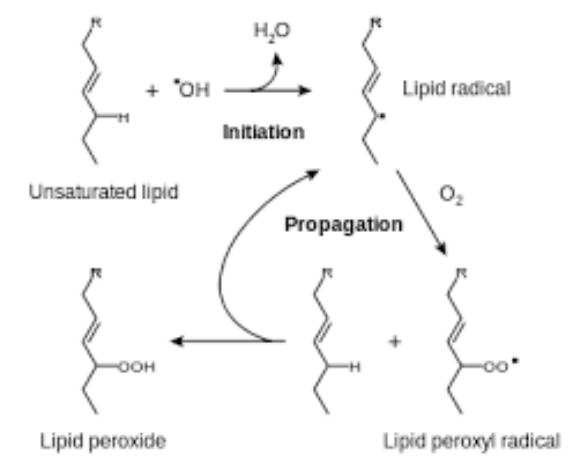
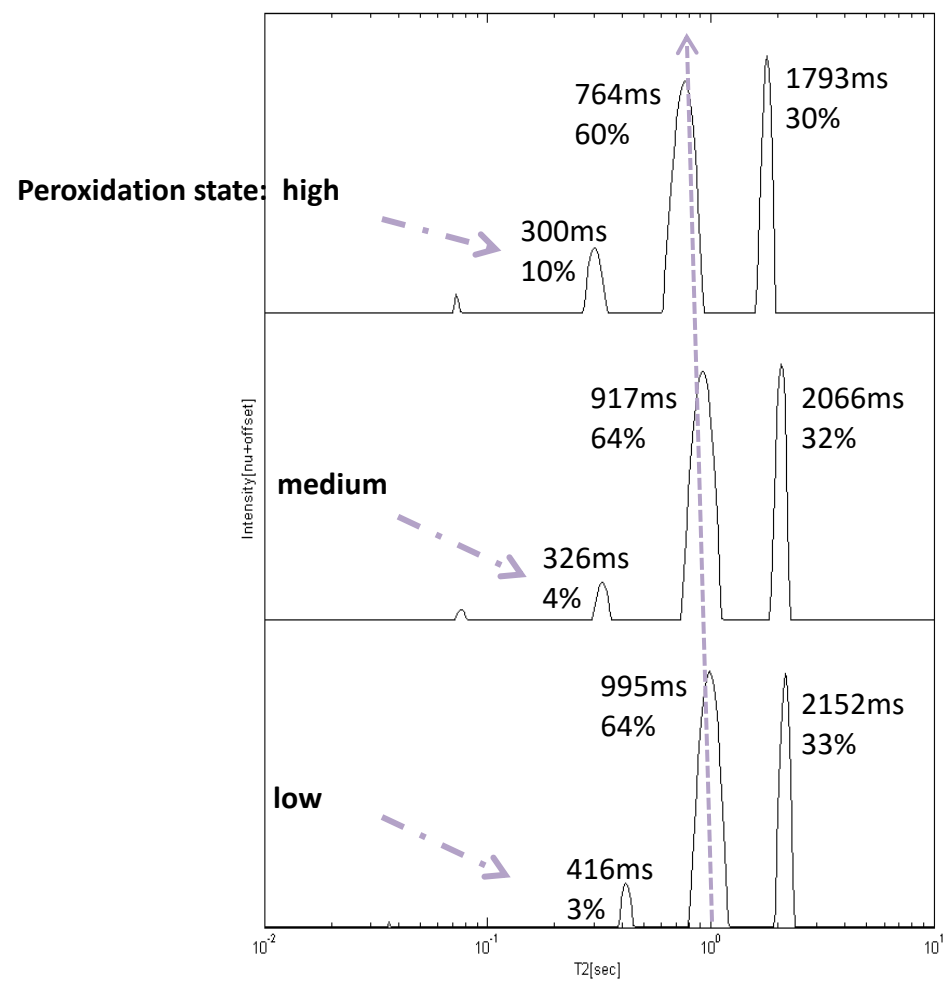
Increased T₂ relaxation times -> Higher Mobility in Magnetic Field

Peak A- Less mobile part of FAMES; Peak B- Mid mobile part; Peak C- Most mobile part/TAIL

Increased T₂ relaxation times -> Lower Viscosity - FLUIDITY

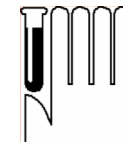


Peroxidation – LF-NMR of 18:3 at 30°C





Biodiesel Standards



Properties	ASTM D6751 B100	EN 14214 B100	EN 590 ULSD
Physical Properties			
Kinematic viscosity, at 40°C, mm ² /s	1.9-6.0	3.5-5.0	2-4.5
Cetane number	47 min.	51 min.	51 min.
Oxidative stability, 110°C, hr	3 min.	6 min.	20 min.
Distillation Temp. (90% vol. recovered), °C	360 max.	-	-
Distillation Temp. (% v/v recovered at 250 °C), °C	-	-	<65 max.
Distillation Temp. (% v/v recovered at 350 °C), °C	-	-	85 min.
Distillation Temp. (95% vol. recovered), °C	-	-	360 max.
Cloud point, °C	Report	Report	Report
Cold filter plugging point, °C	-	Report	Report
Pour point, °C	-	Report	-
Flash point, (closed cup), °C	93 min.	101 min.	55 min.
Density, at 15°C, kg/m ³	-	860-900	820-845
Iodine value, gI/100g	-	120 max.	-
Linolenic acid content, % mol/mol	-	12 max.	-
Content of FAME with > 4 double bonds, % mol/mol	-	1 max.	-
Lubricity, HFRR at 60°C, µm	-	-	460 max.
Elements related to transesterification reaction			
FAME content, % m/m	-	98.5 min.	7 max.
Methanol content, % mol/mol	0.2 max.	0.2 max.	-
Water and sediment, % vol.	0.05 max.	0.05 max.	0.02 max.
Carbon residue, 100% sample, % m/m	0.05 max.	-	-
Carbon residue, 10% distillation residue, % m/m	-	0.3 max.	0.3 max.
Group I metals (Na+K), ppm	5 max.	5 max.	-
Group II metals (Ca+Mg), ppm	5 max.	5 max.	-
Sulfated ash, % m/m	0.02 max.	0.02 max.	0.01 max.
MAG content, % mol/mol	-	0.8 max.	-
DAG content, % mol/mol	-	0.2 max.	-
TAG content, % mol/mol	-	0.2 max.	-
Free Glycerine, % mol/mol	0.02 max.	0.02 max.	-
Total Glycerine, % mol/mol	0.24 max.	0.25 max.	-
Total contamination, mg/kg	-	24 max.	24 max.
Carryover elements			
Copper strip corrosion	No. 3 max.	Class 1	Class 1
Sulfur content, ppm	15 max.	10 max.	10 max.
Acid number, mg KOH/g	0.5 max.	0.5 max.	-
Phosphorus content, % m/m	0.001 max.	0.004 max.	-
Polycyclic aromatic hydrocarbons, % m/m	-	-	11

The various parameters specified in standards can be divided into **oil/petrodiesel physical properties**, and **process-related properties**.

The first category comprises of parameters that largely depend on the **FA/FAME** composition of the chosen oil or quality of the petrodiesel fuel.

The second category can be controlled by changing the **reaction conditions**.



Oil/FAME Related Physical Properties



FAME	CN ¹	MP ¹ [°C]	KV ¹ (40 °C) [mm ² /s]	OS ¹ [h]	BP ² (1 torr) [°C]	SG ³ (15.5 °C) [kg/m ³]	Lubricity ⁴ [μm]
Methyl Palmitate (16:0)	85.9	30	4.38	>24	139	867	360
Methyl Stearate (18:0)	101	39	5.85	>24	155	867	300
Methyl Oleate (18:1)	59.3	-19.5	4.51	2.79	154	878	316
Methyl Linoleate (18:2)	38.2	-35	3.65	0.94	150	890	228
Methyl Linolenate (18:3)	22.7	-52	3.14	0	-	-	184
Methyl Ricinoleate (18:1-OH)	37.38	-5.85	15.29	0.67	177	-	183

CN, Cetane Number; MP, Melting Point; KV, Kinematic Viscosity; OS, Oxidative Stability; BP, Boiling Point; SG, Specific Gravity

¹Knothe, 2008

²Husain et al., 1993

³Clements, 1996

⁴Knothe and Steidly, 2005

FAME Composition (wt %) of Canola (CME), Palm (PME), and Soybean (SME)



	CME	PME	SME
C12:0		0.3	
C14:0		1.1	
C16:0	4.6	41.9	10.5
C18:0	2.1	4.6	4.1
C20:0	0.7	0.3	
C22:0	0.3		
C16:1	0.2	0.2	
C18:1	64.3	41.2	24.1
C18:2	20.2	10.3	53.6
C18:3	7.6	0.1	7.7
Σ SFAME ^a	7.7	48.2	14.6
Σ UFAME ^b	92.3	51.8	85.4

Fuel Properties of CME, PME, and SME and Comparison with ASTM D6751&EN 14214

	ASTM D6751	EN 14214	CME	PME	SME
CN	47 min	51 min	48–56	62 ^b	48–56
ΔH (kJ kg ⁻¹)			37300–39870	37400–38320 ^c	39720–40080
CP (°C)	report		0 ± 1	17 ± 1	1 ± 1
PP (°C)			-9 ± 1	15 ± 1	0 ± 1
CFPP (°C)		variable ^d	-7 ± 1	12 ± 1	-4 ± 1
OSI (h)	3 min	6 min	6.4 ± 0.1	10.3 ± 0.1	5.0 ± 0.1
v (mm ² s ⁻¹)	1.9–6.0	3.5–5.0	4.42 ± 0.23	4.58 ± 0.01	4.12 ± 0.01
lub (μm)			169 ± 1	126 ± 1	136 ± 3
AV (mg of KOH g ⁻¹)	0.50 max	0.50 max	0.01 ± 0.01	0.01 ± 0.01	0.04 ± 0.01
IV		120 max	110	54	134

Moser B.R., 2008. Influence of blending canola, palm, soybean, and sunflower oil FAME on fuel properties of biodiesel. *Energ. Fuel* 22: 4301–4306.

Transesterification process related Properties



Properties	ASTM D6751 B100	EN 14214 B100
Properties related to transesterification reaction		
FAME content, % m/m	-	98.5 min.
Methanol content, % mol/mol	0.2 max.	0.2 max.
Water and sediment, % vol.	0.05 max.	0.05 max.
Group I metals (Na+K), ppm	5 max.	5 max.
Group II metals (Ca+Mg), ppm	5 max.	5 max.
Sulfated ash, % m/m	0.02 max.	0.02 max.
MAG content, % mol/mol	-	0.8 max.
DAG content, % mol/mol	-	0.2 max.
TAG content, % mol/mol	-	0.2 max.
Free Glycerine, % mol/mol	0.02 max.	0.02 max.
Total Glycerine, % mol/mol	0.24 max.	0.25 max.
Total contamination, mg/kg	-	24 max.



•**Total Glycerine = Free Glycerine+ 0.255MAG + 0.146DAG +0.103TAG**

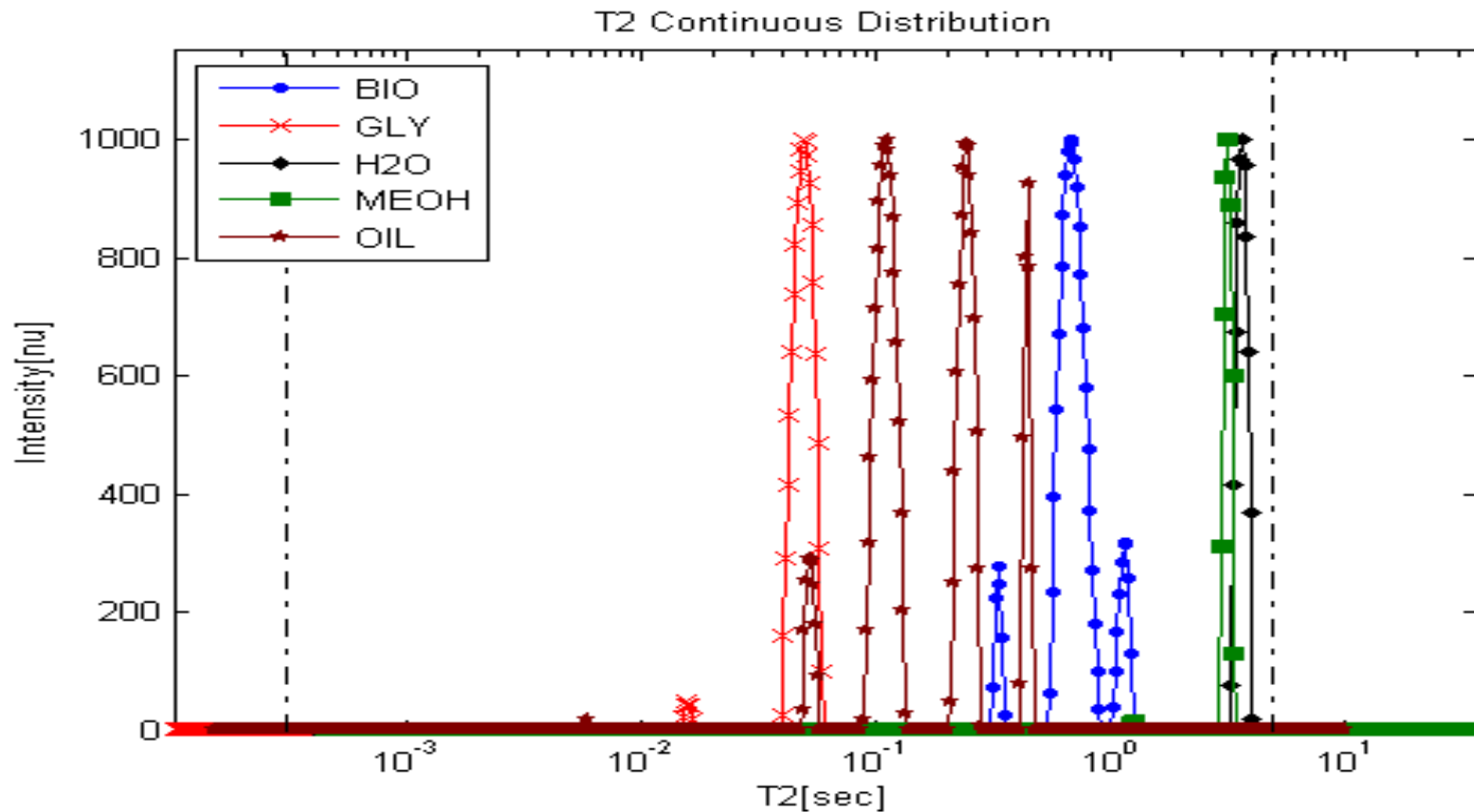
Both standards require the use of traditional Gas Chromatograph (GC) technique.

GC requires the completion of the reaction followed by tedious purification and preparation protocols.

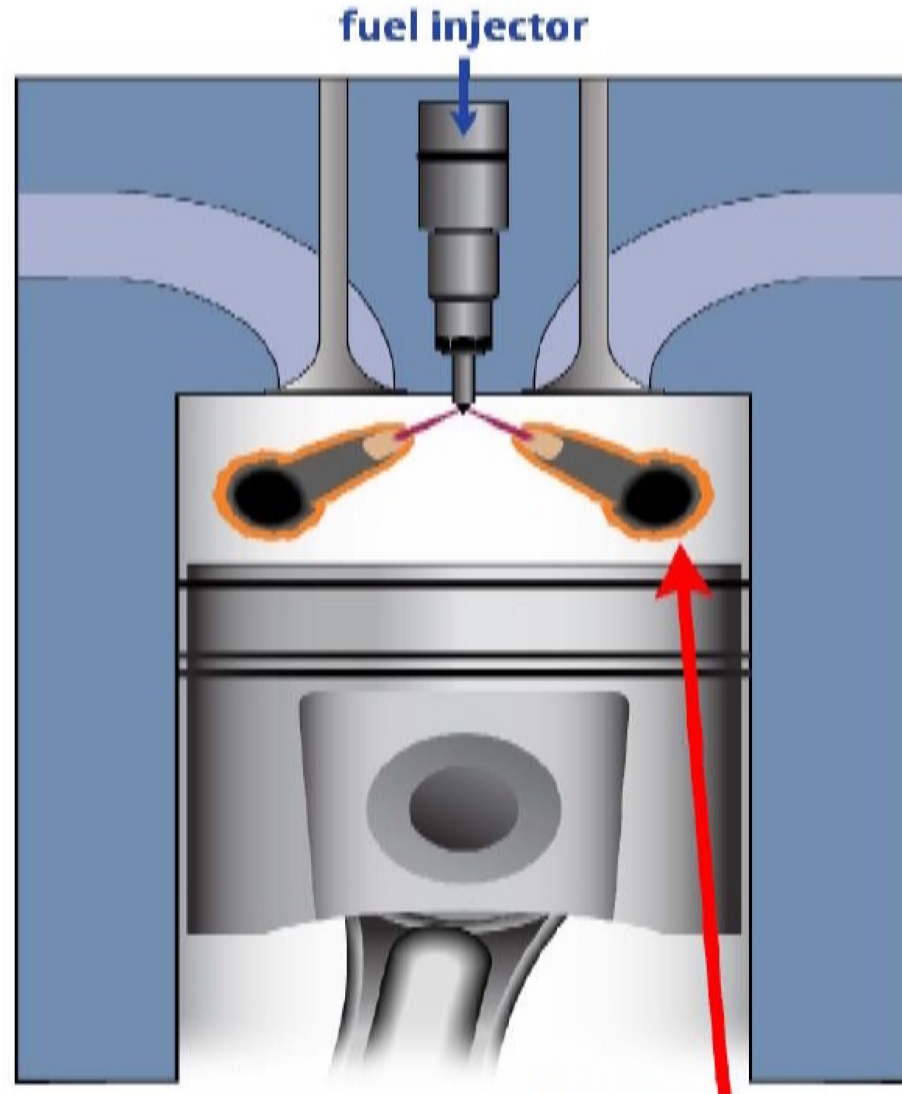
LF-NMR Monitoring of TE

LR-NMR advantages: Non-destructive; rapid; accurate; reliable and low cost detection.

* Low resolution **is limited** to distinguish between species **but** is **sufficient** to differentiate between **classes of components**.



Diesel Engine (Compression Ignition)



**Hot-Flame Region:
NO_x & Soot**

Combustion & Emission - Parameters in Focus:

Flow

Liquid FAME viscosity

Phase transition

Liquid FAME

Distillation/Vaporisation

NO_x

Oxygen Content/Stability

FAME Self Organization – Packaging

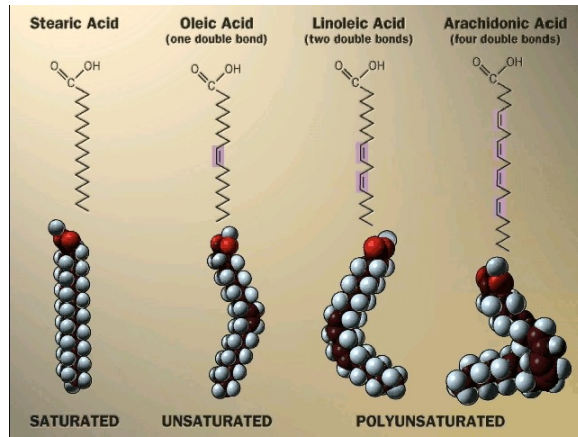
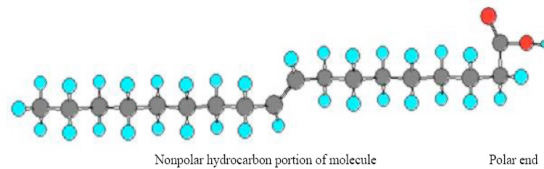
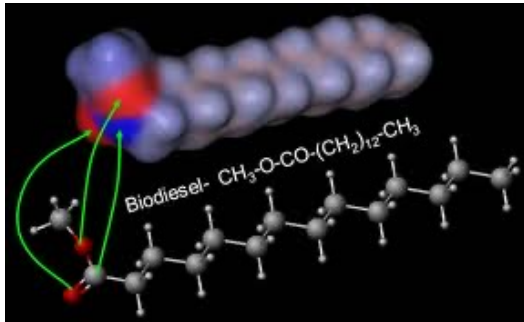
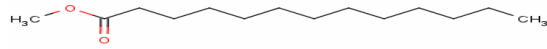
Analytical Study Tools:

Spectroscopy (NMR; FTIR;
Raman)

XRD

Microscopy (SEM; TEM)

Flow - Viscosity



FAME profiles and calculated viscosities of 6 biodiesels samples

Sample ^a	FAME composition ^b [%]									Calculated C _{18:1} - viscosities [mm ² /s]
	C _{16:0}	C _{18:0}	C _{18:1}	C _{18:2}	C _{18:3}	C _{20:0}	C _{20:1}	C _{22:1}	OH	
Linseed	5.6	4.6	18.2	15.4	56.1	-	-	-	-	3.60
Soy	10.8	3.6	25.6	53.4	5.5	0.4	0.4	0.4	-	3.99
Canola	4.8	1.6	63.7	20.3	7.2	0.6	1.3	-	-	4.25
Olive	10.6	2.8	77.3	7.4	0.6	0.4	-	-	-	4.45
Mustard	1.7	1.0	9.8	13.8	12.9	0.8	6.2	51.4	-	5.52
Castor	1.0	1.1	3.0	3.9	-	-	-	-	91.1	13.76

